

# CHIMIA

---

CHIMIA 2014, Volume 68  
ISSN 0009-4293  
[www.chimia.ch](http://www.chimia.ch)



SCS  
Swiss Chemical  
Society

Supplementa to Issue 7-8/2014

## SCS Fall Meeting 2014 Poster Abstracts Session of Physical Chemistry

September 11, 2014  
University of Zurich, Irchel Campus  
<http://scg.ch/fallmeeting2014>

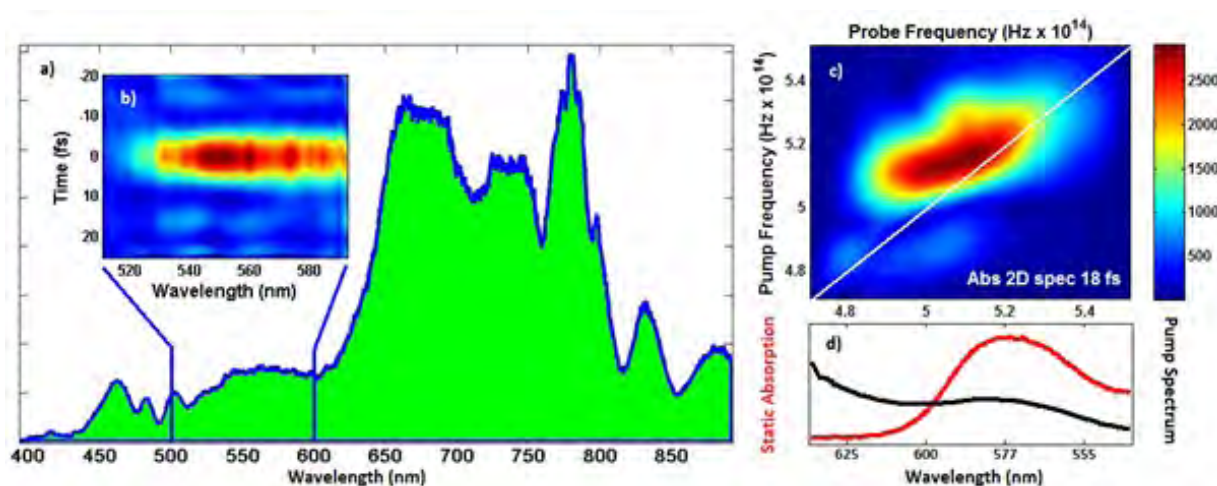
Swiss Chemical Society  
Schwarztorstrasse 9  
3007 Bern  
Switzerland  
[info@scg.ch](mailto:info@scg.ch)  
[www.scg.ch](http://www.scg.ch)

## Ultra-Broadband Multidimensional Electronic Spectroscopy Setup

Andre Al Haddad<sup>1</sup>, Adrien Chauvet<sup>1</sup>, Majed Chergui<sup>1</sup> \*

<sup>1</sup>EPFL Lausanne

Coherent electronic spectroscopy is a powerful technique to resolve electronic correlations between different transitions or initial and final states in molecular systems. Studying complex systems requires addressing several electronic states simultaneously, which often means that the experiments have to be performed with a large spectral bandwidth. Here we present a compact passively phase stabilized ultra-broadband 2D Fourier transform setup using conventional optics in the visible range. A gas filled hollow core fiber pumped by an amplified Ti:Al<sub>2</sub>O<sub>3</sub> laser is used as a light source. It provides a spectral range from 420 to 750 nm (fig. 1 a) with sufficient intensity to allow compression using a pulse shaper; pumping the fiber with the second harmonic gives access to a spectral range of 370 to 480 nm. Currently a visible bandwidth of 90 nm, compressed via a deformable mirror based pulse shaper to sub-10 fs pulses (fig. 1 b), is used.



The advantages of the hollow core fiber, compared to conventionally used NOPAs, reside in a flatter spectrum over a large spectral range, no spatial chirp of the output beam, and high output intensity allowing the easy use of pulse shapers. Phase correction of the 2D data is performed via transient pump-probe measurements done on the same setup. Primary broadband measurements on a dye (Rhodamine 101) will be presented. We report an oscillation of the ellipticity and intensity of the 2D spectra.

## High resolution THz spectroscopy between 0.8 and 3 THz with a Synchrotron source and a Bruker interferometer.

Sieghard Albert<sup>1</sup>, Sigurd Bauerecker<sup>2</sup>, Philippe Lerch<sup>3</sup>, Martin Quack<sup>1</sup>, Alexander Wokaun<sup>4</sup> \*

<sup>1</sup>Physical Chemistry, ETH Zürich, CH-8093 Zürich, <sup>2</sup>Institute for Physical Chemistry, TU Braunschweig, D-38106, Germany, <sup>3</sup>Swiss Light Source, Paul-Scherrer-Institute, CH-5332 Villigen, <sup>4</sup>Energy Research Department, Paul-Scherrer-Institute, CH-5232 Villigen

One of the great challenges of modern high resolution spectroscopy is to find devices which cover the THz gap between 0.7 and 5 THz. We have extended our high resolution FTIR setup at the Swiss Light Source described in Ref. [1-4] with a collisional cooling multireflection cell which makes it possible to record spectra down to 850 GHz ( $28\text{ cm}^{-1}$ ). Due to the high brightness of the synchrotron radiation the signal-to-noise ratio is effectively 20 to 50 times better than that of conventional thermal sources in the spectral region below 4 THz. Our resolution is in the order of 15 MHz which makes it possible to measure rotational spectra. Using the collisional cooling method we are able to measure at low temperature down to 80 K or even 10 K. In order to demonstrate the resolving power and the excellent signal-to-noise ratio of our FTIR setup we shall present the rotational spectra of CO, deuterated methanes and the rovibrational spectra of aromatic compounds with low lying modes in the range 0.8 THz to 3 THz. Work supported by ETH, SNF, ERC and SLS.

[1] S. Albert, K. K. Albert, P. Lerch, M. Quack, *Faraday Discuss.* **2011**, 150, 71-99.

[2] S. Albert, K. Keppler Albert, M. Quack, in *Handbook of High Resolution Spectroscopy, Vol. 2* (Eds.: M. Quack, F. Merkt), John Wiley Sons, Ltd, Chichester, **2011**, pp. 965-1019.

[3] S. Albert, Ph. Lerch, M. Quack, *ChemPhysChem* **2013**, 14, 3204-3208.

[4] S. Albert, Ph. Lerch, R. Prentner, M. Quack, *Angew. Chem. Int. Ed.* **2013**, 52, 346-349.

## Off-axis deflection and Rydberg-Stark deceleration of a supersonic beam of H<sub>2</sub> molecules on a printed circuit board

Pitt Allmendinger<sup>1</sup>, Johannes Deiglmayr<sup>1</sup>, Josef Anton Agner<sup>1</sup>, Hansjürg Schmutz<sup>1</sup>, Frédéric Merkt<sup>1</sup> \*

<sup>1</sup>Laboratory of Physical Chemistry, ETH Zurich, 8093 Zurich, Switzerland

With the goal of investigating low-energy collisions between Rydberg atoms or molecules and ground state atoms and molecules, we have developed a bent surface-electrode Rydberg-Stark decelerator. The decelerator design is an extension of linear surface-electrode decelerators for polar molecules [1] and Rydberg atoms [2,3]. With this decelerator, we can deflect the Rydberg atoms or molecules from the propagation axis of a supersonic beam. The deflection can be carried out simultaneously with a deceleration of the beam, which enables us to generate velocity tunable samples of translationally cold ( $T_{\text{trans}}=200$  mK) atoms and molecules. The operational principle of this new device will be illustrated by a series of imaging measurements in which we have detected and characterized a beam of cold H<sub>2</sub> molecules after deflection and deceleration. The advantage of this deceleration method compared to deceleration along the axis of a supersonic beam is that collisions with undecelerated particles do not reduce the phase-space density of the decelerated sample. Moreover, it enables us to study collisional processes without interference from these undecelerated particles. This advantage will be illustrated in a study of collisions between  $n \approx 30$  H<sub>2</sub> Rydberg molecules and H<sub>2</sub> ground state molecules.

[1] S. A. Meek, H. L. Bethlem, H. Conrad, and G. Meijer, *Phys. Rev. Lett.*, **2008**, 100, 153003

[2] S. D. Hogan, P. Allmendinger, H. Saßmannshausen, H. Schmutz and F. Merkt, *Phys. Rev. Lett.*, **2012**, 108, 063008

[3] P. Allmendinger, J. A. Agner, H. Schmutz and F. Merkt, *Phys. Rev. A.*, **2013**, 88, 043433

**Photoelectron spectroscopy of liquid phase benzene derivatives.**

Christopher Arrell<sup>1</sup>, Jose Ojeda<sup>1</sup>, Lars Mewes<sup>1</sup>, L. Miseikis<sup>2</sup>, A Sanchez-Gonzalez<sup>2</sup>, T. Witting<sup>2</sup>,  
Majed Chergui<sup>1</sup> \*

<sup>1</sup>EPFL Lausanne, <sup>2</sup>Imperial College

Liquid phase photoelectron spectroscopy (LPES) using monochromatic high harmonic radiation (VUV) has been used for the first time to directly measure the first nine molecular orbitals of 1,3,5 trimethybenzene (mesitylene), 1,2,3 trimethybenzene, 1,2,4 trimethybenzene, o-Xylene and m-Xylene. Spectra were taken using a micro liquid jet to create a 20  $\mu\text{m}$  diameter jet of laminar flow in high vacuum conditions and a differentially pumped time-of-flight electron spectrometer developed at the LSU, EPFL. The high-harmonic beamline at the Artemis facility, Rutherford Appleton labs in the UK was used as a photon source, delivering 30 eV monochromatic (0.2 eV FWHM) photons. To obtain liquid phase spectra, first the VUV probe was aligned to collect gas phase only spectra close to the liquid jet, before the VUV was aligned onto the liquid jet. In this position both gas and liquid phase spectra were collected, requiring the initial gas-only spectra to be subtracted to yield the liquid only spectra. Interestingly a near uniform relaxation of all binding energies was observed for the liquid phase spectra compared to the gas phase for all derivatives of  $\sim 0.8$  eV. This shift has previously been reported by Kock and co-workers<sup>1</sup> of benzene layers absorbed onto Ag substrates. Anisotropy measurements revealed a reduction of anisotropy in the liquid phase compared to gas phase as expected.

[1] R. Dudde, E-E Koch, *Surface Science*, **1990**, 225, 267-272

**(Benzene)<sub>2</sub> and (Benzonitrile)<sub>2</sub>: Excitonic and Site Effects on the S<sub>1</sub>/S<sub>2</sub> Splitting**Franziska Balmer<sup>1</sup>, Maria Trachsel<sup>1</sup>, Philipp Ottiger<sup>1</sup>, Samuel Leutwyler<sup>1</sup> \*<sup>1</sup>University of Berne

The substitution of a hydrogen atom in a benzene molecule by a cyano group, forming benzonitrile, causes strong changes in the dimerization behaviour of the molecule. While the benzene dimer (Bz)<sub>2</sub> is a C<sub>s</sub>-symmetric T-shaped dimer forming a CH<sup>⋯</sup>π bond, benzonitrile forms a planar C<sub>2h</sub>-symmetric dimer (BN)<sub>2</sub> with two equivalent antiparallel CN<sup>⋯</sup>H hydrogen bonds [1]. (Bz)<sub>2</sub> and (BN)<sub>2</sub> were studied by mass-resolved two-color resonant two-photon ionization spectroscopy in a supersonic jet and by means of ab-initio and density functional methods. In each case, spectra of the dimers and their partially deuterated and <sup>13</sup>C-isotopomers were recorded and interpreted.

In (Bz)<sub>2</sub>, the S<sub>1</sub>/S<sub>2</sub> splitting is dominated by the inequivalence of its monomers. While the S<sub>2</sub>←S<sub>0</sub> transition of (Bz)<sub>2</sub> is very weak, the site splitting was determined to be between 200 - 220 cm<sup>-1</sup>.

(BN)<sub>2</sub> is an excitonic dimer. Its S<sub>1</sub>←S<sub>0</sub> transition is symmetry-forbidden (<sup>1</sup>A<sub>g</sub>←<sup>1</sup>A<sub>g</sub>), and the S<sub>2</sub>←S<sub>0</sub> transition (<sup>1</sup>B<sub>u</sub>←<sup>1</sup>A<sub>g</sub>) is observed at 36420 cm<sup>-1</sup> [1]. In the <sup>13</sup>C-isotopomer the monomers are inequivalent, rendering the S<sub>1</sub>←S<sub>0</sub> transition allowed. The S<sub>1</sub>/S<sub>2</sub> splitting of the <sup>13</sup>C-isotopomer is 3.9 cm<sup>-1</sup> and consists of an excitonic contribution (2.0 ± 0.2 cm<sup>-1</sup>) and a <sup>13</sup>C-isotope effect (3.3 ± 0.1 cm<sup>-1</sup>).

[1] M. Schmitt, M. Böhm, C. Ratzer, S. Siegert, M. Von Beek, W. L. Meerts, J. Mol. Struct. 795, 2006

## Multichannel quantum defect theory (MQDT) assisted spectroscopy of $H_2^+$ through the Rydberg spectrum of $H_2$ .

Maximilian Beyer<sup>1</sup>, Christa Haase<sup>1</sup>, Christian Jungen<sup>2</sup>, Frédéric Merkt<sup>1</sup> \*

<sup>1</sup>Laboratory of Physical Chemistry, ETH Zurich, 8093 Zurich, Switzerland, <sup>2</sup>Laboratoire Aimé Cotton du CNRS, Orsay Cedex, France

High-resolution spectroscopy of high Rydberg states in combination with Rydberg-series extrapolation methods enable one to determine the vibrational, rotational and even the fine and hyperfine structures of molecular cations [1].

We present recent results on the determination of rotational and spin rotational intervals in para  $H_2^+$  by Rydberg-series extrapolation using MQDT [2, 3]. The principles of the extrapolation will be explained and illustrated by comparison with high-resolution spectroscopy data on Rydberg states of  $H_2$  obtained in the millimeter-wave, sub-millimeter-wave and optical ranges of the electromagnetic spectrum.

The emphasis will be placed on the determination of the spin-rotational fine structure of the lowest vibrational levels of para  $H_2^+$  and of the rovibrational level structure of  $H_2^+$ .

[1] F. Merkt, S. Willitsch and U. Hollenstein (2011) High-resolution Photoelectron Spectroscopy, in *Handbook of High-resolution Spectroscopy*, M. Quack and F. Merkt (eds), John Wiley Sons, Ltd., Chichester, UK.

[2] Ch. Jungen (2011) Elements of Quantum Defect Theory, in *Handbook of High-resolution Spectroscopy*, M. Quack and F. Merkt (eds), John Wiley Sons, Ltd., Chichester, UK.

[3] D. Sprecher, Ch. Jungen and F. Merkt, *J. Chem. Phys.* **140**, 104303:1-18 (2014).

**Energytransfer of Eu<sup>2+</sup> in SrAl<sub>2</sub>O<sub>4</sub> codoped with Dy<sup>3+</sup>**

Jakob Bierwagen<sup>1</sup>, Hans Hagemann<sup>1</sup> \*

<sup>1</sup>University of Geneva

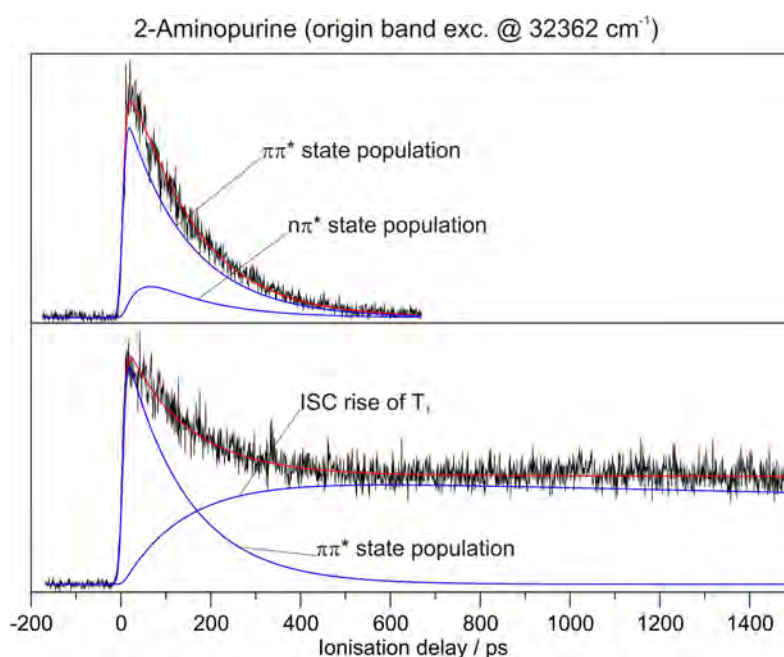
SrAl<sub>2</sub>O<sub>4</sub>, codoped with Eu<sup>2+</sup> and Dy<sup>3+</sup>, is one of the most efficient afterglow materials [1]. In this study we present experimental results on fluorescence lifetime studied as a function of temperature and excitation wavelength to gain more quantitative insight into energy transfer processes in this material. These energy transfers take place between Eu ions on different lattice sites and also from the Eu ions to the conduction band, as shown recently [2].

[1] Matsuzawa T, Apki Y, Takeuchi N, et al., *J. Electrochemistry Society*, **1996**, 143, 2670-2673.

[2] J. Ueda, T Nagkanishi, Y. Katayama and S. Tanabe, *Physica Status Solidi C*, **2012**, 9, 2322-2325

**Excited State Photophysics of Jet-Cooled 2-Aminopurine and 9-Methyl-2-Aminopurine**Susan Blaser<sup>1</sup>, Simon Lobsiger<sup>1</sup>, Hans-Martin Frey<sup>1</sup>, Samuel Leutwyler<sup>1</sup> \*<sup>1</sup>University of Berne

2-Aminopurine (2AP) is a fluorescent analogue of adenine and is often incorporated into DNA to study the structure and dynamics of DNA oligomers. 2AP exhibits a long fluorescence lifetime of  $\tau = 11$  ns in aqueous solution. [1] It is however almost non-fluorescent in the gas phase. [2] The reasons for this difference have been determined by ps pump-ionisation methods. [3] In the excited state 2AP and 9-methyl-2AP undergo efficient  $^1\pi\pi^* \rightarrow ^1n\pi^*$  internal conversion (IC). The  $^1n\pi^*$  state undergoes efficient intersystem crossing (ISC) to the  $T_1$  state and relaxes to the  $S_0$  state via IC. If 2AP is solvated with one  $H_2O$  molecule, the excited state photophysics change radically, depending on the solvation site. [3]

[1] A. Holmén, B. Norden, B. Albinsson, *J. Am. Chem. Soc.*, **1997**, 119, 3114,[2] M. A. Trachsel, S. Lobsiger, T. Schär, S. Leutwyler, *J. Chem. Phys.*, **2014**, 140, 044331[3] S. Lobsiger, R. K. Sinha, S. Blaser, H.-M. Frey, S. Leutwyler, *submitted*

## High Resolution Analysis of the FTIR spectra and quantum dynamics of CHF<sub>3</sub>: The 2ν<sub>4</sub> (A<sub>1</sub>/E) Band

Irina Bolotova<sup>1</sup>, Oleg Ulenikov<sup>2</sup>, Elena Bekhtereva<sup>2</sup>, Sieghard Albert<sup>1</sup>, Hans Hollenstein<sup>1</sup>, Martin Quack<sup>1</sup> \*

<sup>1</sup>Laboratory of Physical Chemistry, ETH Zurich, 8093 Zurich, Switzerland, <sup>2</sup>Tomsk State University, Physics Department, 634050, Tomsk, Russia

CHF<sub>3</sub> is a prototype molecule for the study of intramolecular energy flow<sup>1-4</sup>. Despite a long history<sup>1-9</sup> its rotationally resolved infrared spectrum is poorly understood due to numerous strong interactions. We have reinvestigated the IR spectrum of CHF<sub>3</sub> at highest resolution. Here we present the results of reanalysis of the 2ν<sub>4</sub> band, located between a 2650 and 2850 cm<sup>-1</sup>, previously investigated at lower resolution<sup>3,5</sup>. The band is known as being involved in a Fermi resonance with the stretching fundamental ν<sub>1</sub>, which is an essential doorway to intramolecular vibrational redistribution<sup>9</sup>.

The high resolution FTIR spectrum of CHF<sub>3</sub> has been measured with the Bruker 125 HR Zürich Prototype spectrometer using a White cell with the optical path length of 19.2 meters at room temperature. As a result of the analysis, transitions up to J<sub>max</sub> = 30 have been assigned for the symmetric component A<sub>1</sub> of 2ν<sub>4</sub> band, and J<sub>max</sub> = 60 for the 2ν<sub>4</sub> (E) band. The new analysis results in a set of effective Hamiltonian parameters, which reproduce the experimental data with an accuracy close to the experimental uncertainties.

Our work is supported by ETHZ, SNF and ERC.

[1] S. Albert, K. Keppler Albert, H. Hollenstein, C. Manca Tanner, and M. Quack in **Handbook of High Resolution Spectroscopy**, Vol. 1, p.117-173; S. Albert, K. Keppler Albert, and M. Quack, Vol. 2, p.965-1019, M. Quack and F. Merkt eds., Wiley Chichester 2011.

[2] H. R. Dübal, and M. Quack, *Chem. Phys. Lett.*, **1981**, 80, 439 - 444.

[3] H. R. Dübal, and M. Quack, *J. Chem. Phys.*, **1984**, 81, 3779 - 3791.

[4] R. Marquardt, M. Quack, J. Stohner and E. Sutcliffe, *J. Chem. Soc., Faraday Trans.*, **1986**, 82, 1173 - 1187.

[5] A. S. Pine, and J. M. Pliva, *J. Mol. Spectrosc.*, **1988**, 130, 431 - 444.

[6] J. Segall, R. N. Zare, H. R. Dübal, M. Lewerenz, and M. Quack, *J. Chem. Phys.*, **1986**, 86, 634 - 646.

[7] A. Amrein, M. Quack, and U. Schmitt, *Mol. Phys.*, **1987**, 60, 237 - 248.

[8] A. Amrein, M. Quack, and U. Schmitt, *J. Phys. Chem.*, **1988**, 92, 5455 - 5466.

[9] M. Quack, *Annu. Rev. Phys. Chem.*, **1990**, 41, 839 - 874.

**Effect of Ba and K addition and controlled spatial deposition of Rh in Rh/Al<sub>2</sub>O<sub>3</sub> catalysts for CO<sub>2</sub> hydrogenation**

Robert Büchel<sup>1</sup>, Sotiris E. Pratsinis<sup>1</sup>, Alfons Baiker<sup>1</sup> \*

<sup>1</sup>ETH Zurich

The effect of Ba and K addition to Rh/Al<sub>2</sub>O<sub>3</sub> catalysts for CO<sub>2</sub> hydrogenation was investigated. Catalysts with preferential deposition of 1 wt% Rh either on the alumina support or the Ba or K component was prepared by the two nozzle flame spray pyrolysis method. The pure Rh/Al<sub>2</sub>O<sub>3</sub> catalyst as well as the Ba-containing catalysts showed a high selectivity to CH<sub>4</sub> below 500 °C with a maximum yield at 400 °C; Above 400 °C, the reverse water gas shift reaction leading to CO and H<sub>2</sub>O started to become dominant, in accordance with thermodynamics. In contrast, the K-containing catalysts produced no CH<sub>4</sub>, all CO<sub>2</sub> was directly converted to CO in the entire temperature range (300-800 °C). Preferential deposition of the Rh on the additive components (Ba, K) or the alumina support had comparably little effect on the catalytic behavior. The catalysts were characterized by nitrogen adsorption, CO chemisorption combined with diffuse reflectance infrared Fourier transform spectroscopy (DRIFTS), and scanning transmission electron microscopy. XRD and thermoanalysis combined with mass spectroscopy indicated that the Ba existed mainly as BaCO<sub>3</sub>, while K was present in the form of KHCO<sub>3</sub> and KOH. DRIFTS combined with CO adsorption measurements revealed a strikingly different CO adsorption behavior of Ba- and K-containing catalysts.

## Plasmon tuning of gold nanoparticles array for surface enhanced Raman scattering

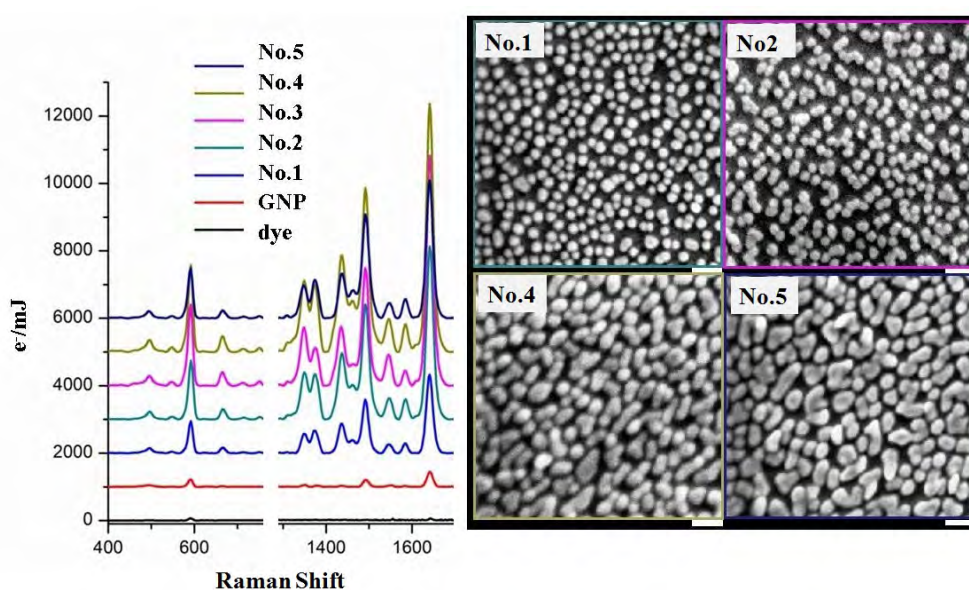
Mahshid Chekini<sup>1</sup>, Patric Oulevey<sup>1</sup>, Thomas Bürgi<sup>1</sup> \*

<sup>1</sup>University of Geneva

Raman spectroscopy is a promising tool for molecular sensing. Inherently small scattering cross sections can be compensated by signal enhancement at metal surfaces due to the localized electromagnetic field. However, bottom-up fabrication of uniform, large scale and reproducible templates for Raman enhancement is crucial but challenging.

In this study we present a facile method to fabricate uniform, tunable plasmonics-based templates for Raman signal enhancement. We used a cationic polyelectrolyte to self assemble gold nanoparticles on large-scale glass surface. We then modified the particles by several controlled growing steps, which lead to a shift of the plasmon resonance. The induced local electric field in gold nanoparticles due to their plasmon resonance excitations has an amplifying effect on Raman scattering of the analyte close to the particles. Furthermore, depending on the particle distances, the plasmon resonances between neighboring particles are coupled with each other. This allows more tuning of the plasmon resonances for optimal Raman signal amplification.

Several templates were fabricated to study a Raman active Nile-blue A fluorophore, by UV-Vis, and Raman spectroscopy with three different excitation laser lines. The results from the latter technique showed a noticeable enhancement due to the nanoparticles' plasmonic-tuning with excitation laser line in presence of optimal growth step. Furthermore the nanostructure characteristics of the templates were investigated by scanning electron microscopy. As it presented in following figure (scale bar 100 nm), applying the growing steps led to increase of nanoparticle sizes and change of inter-particle distances. By applying 4 and 5 steps of growing, we observed red shifted plasmon resonance to NIR and the aggregation of the closest neighbors into larger and more elongated particles via the SEM micrographs. Preliminary attempts were also done on flexible substrates by applying a mechanical stress for plasmonic-tuning.

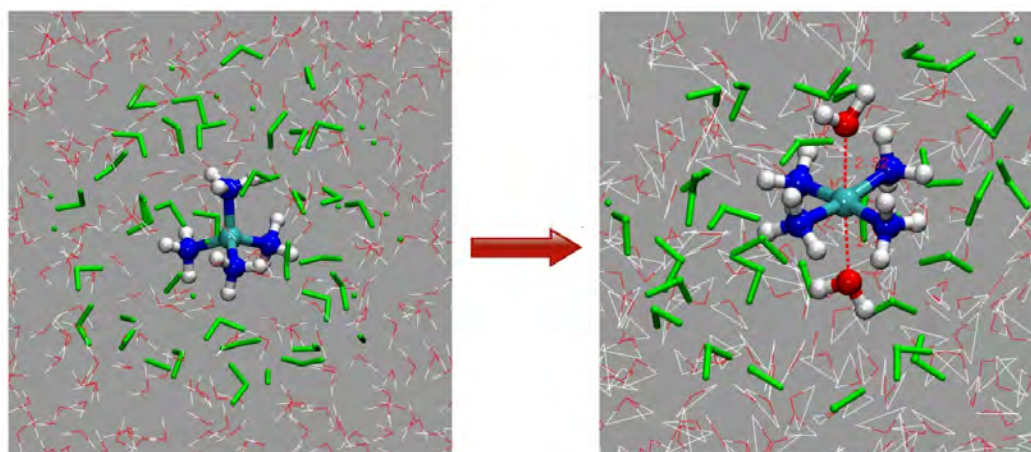


## Solvation Dynamics Around Photo-excited Transition Metal Complexes: A Molecular Dynamics Approach

Akshaya Das<sup>1</sup>, Markus Meuwly<sup>1</sup> \*

<sup>1</sup>University of Basel

Understanding the details of the structural rearrangement of solvent molecules around photo-excited transition metal (TM) complexes gains increased interest in the recent past because of the importance of such systems in solar energy conversion. Following our previous work on Ru and Fe complexes, we studied the structure and dynamics of solvent shells around photo-excited  $[\text{Cu}(\text{NH}_3)_4]^{\text{+1}}$  (tetrahedral) to  $[\text{Cu}(\text{NH}_3)_4]^{\text{+2}}$  (square planer) complexes using the VALBOND-TRANS (VBT) force field together with molecular dynamics (MD) simulations. We also performed QM/MM hybrid MD simulation using SCC-DFTB to investigate the photo excitation process in  $[\text{Cu}(\text{NH}_3)_4]^{\text{+1}}$  complex. Electronic excitation of Cu(I) to Cu(II) brings the system to a non-equilibrium state in which the excess energy is redistributed to the surrounding solvent molecules. In the preliminary stage, we found that the structural change tetrahedral to square planer in going from Cu(I) to Cu(II) occurs in the picoseconds time scale. The time dependent radial distribution of water molecules was evaluated to characterize the structural rearrangement of solvent molecules in the vicinity of the metal center. In order to validate our force field, IR spectrum of  $[\text{Cu}(\text{NH}_3)_4]^{\text{+1}}$  was computed and compared with the experimental peaks.



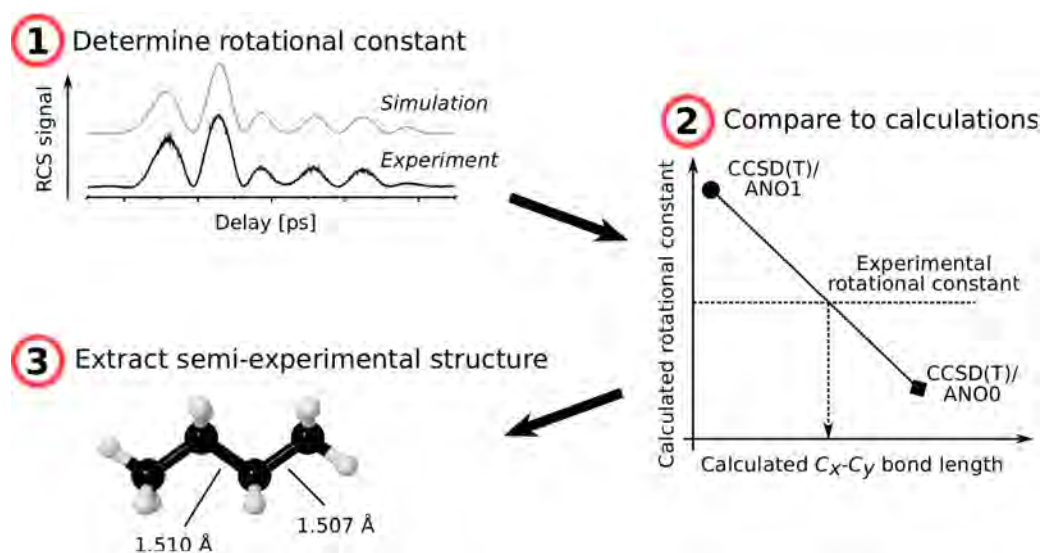
- [1] T. J. Penfold et al., *J. Phys. Chem. A*, **2013**, 117, 4591-4601
- [2] L. M. L. Daku et al., *J. Phys. Chem. Lett.*, **2010**, 1, 1830-1853
- [3] K. Haldrup et al., *J. Phys. Chem. A*, **2012**, 116, 9878-9887
- [4] J. J. Szymczak et al., *Phys. Chem. Chem. Phys.*, **2013**, 15, 6268-6277

## Structure of n-Alkanes

Takuya Den<sup>1</sup>, Philipp Kowalewski<sup>1</sup>, Hans-Martin Frey<sup>1</sup>, Samuel Leutwyler<sup>1</sup> \*

<sup>1</sup>University of Berne

*n*-Alkanes are discussed within the first hundred pages of every freshman chemistry textbook. Surprisingly, the gas-phase structure of these molecules has never been determined with high precision. Structure determination by microwave spectroscopy is not possible, as *n*-alkanes possess only very small or zero dipole moments. In contrast to classical methods, femtosecond time-resolved rotational coherence spectroscopy (RCS) does not require a dipole moment. This non-linear four-wave mixing method allows to probe the rotation of non-polar gas-phase molecules on the femtosecond time scale, thereby giving accurate rotational constants. We used RCS to determine ground-state rotational constants of the *n*-butane, *n*-pentane, *n*-hexane, *n*-heptane and *n*-octane. By comparing the experimental rotational constants with *ab-initio* calculations, a semi-experimental determination of C-C bond lengths is possible.



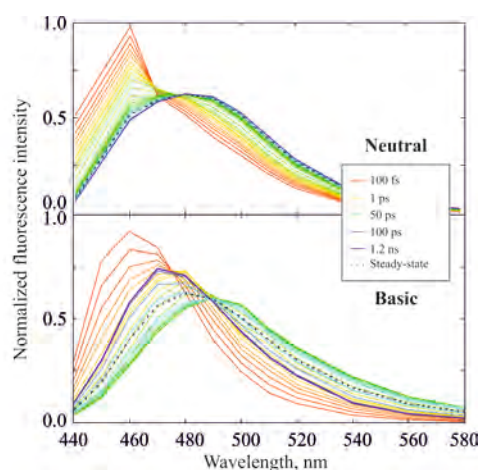
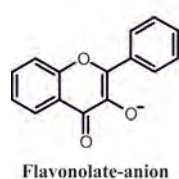
**Ultrafast excited-state dynamics of flavonol anion: no intermolecular proton transfer**

Bogdan Dereka<sup>1</sup>, Romain Letrun<sup>1</sup>, Denis Svechkarev<sup>1</sup>, Arnulf Rosspeintner<sup>1</sup>, Andrey O. Doroshenko<sup>2</sup>, Eric Vauthey<sup>1</sup> \*

<sup>1</sup>University of Geneva, <sup>2</sup>Kharkov V. N. Karazin National University

Flavonols are widely known for their rich photochemistry and photophysics in the excited state due to the occurrence of ESIPT (Excited-State Intramolecular Proton Transfer). However, even for the parent flavonol molecule, its photocycle is not completely understood in polar and hydrogen-bonded systems. The photophysics of the flavonolate-anion has been attracting attention over the last years due to its omnipresence in biological, aqueous and alcohol systems containing flavonol. Being the simplest system in the flavonoid family, it forfeits the intramolecular proton transfer process in the  $S_1$  state, but it is available for an intermolecular proton transfer reaction from surrounding proton-donating molecules in the excited state.

We investigated the behaviour of the flavonolic anion in its  $S_1$  state using a combination of steady-state and time-resolved techniques including transient absorption in UV-visible and infrared ranges and time-resolved fluorescence in femto- to nanosecond time domain. We showed that the excited-state lifetime of flavonolate-anion widely accepted in literature (2.2 ns) corresponds to another species existing in traceable quantities in alcohol solutions, whose contribution strongly depends on the pH. We tentatively assume it to be a hydrogen-bonded complex of the parent flavonol with the solvent. The actual lifetime of the anionic form is significantly shorter (35-45 ps) and occurs on a similar timescale as solvent relaxation. The time evolution of emission spectrum is shown below for neutral and basic solutions of flavonol in methanol under selective anion excitation. Intermolecular proton transfer reaction in the excited state of the anion does not occur even in strongly hydrogen-bonding donating solvents, such as water or methanol. A solvent relaxation involving intramolecular vibrational modes is found to be the only process in the excited state of the flavonolic anion.



## Signal Enhancement Artifacts Suppression in Vibrational Circular Dichroism Spectroscopy with Femtosecond Lasers

Biplab Dutta<sup>1</sup>, Jan Helbing<sup>1</sup> \*

<sup>1</sup>University of Zurich

Vibrational Circular Dichroism (VCD) Spectroscopy is an important tool to resolve the configuration and conformation of chiral molecules in solution. The goal of our work to extend this technique to time resolved measurements<sup>1</sup> with femtosecond resolution of the laser. Despite the high sensitivity of laser based experiments, always suffers from different polarization artifacts and large achiral background contributions whereas the changes in chiral signal<sup>2</sup> are  $10^{-5}$  to  $10^{-6}$ . To circumvent these problems, we will discuss our interferometer based approach to detect & enhance VCD signal<sup>2</sup> as well as artifacts suppression. Simulation of the VCD signal with different artifacts (circular birefringence, linear birefringence and linear dichroism, chirp) and polarizer extinction coefficient will be discussed. Comparison with existing approaches will also be provided.

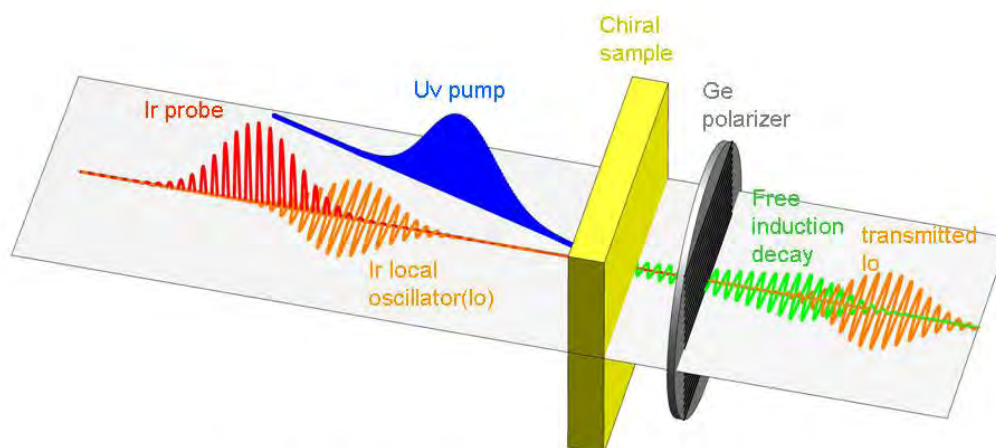


Fig:Schematic of time resolved VCD detection

[1] Mathias Bonmarin, Jan Helbing. *Optics Letters*, **2008**, 33, 2086-2088.

[2] Mathias Bonmarin, Jan Helbing. *J Chem Phys*, **2009**, 131, 174507-1- 174507-9.

## Controlled Chemistry using Cold Atomic or Molecular Ions and Ultracold Atoms in Hybrid Traps

Pascal Eberle<sup>1</sup>, Ravi Krishnamurthy<sup>1</sup>, Maurice Raoult<sup>2</sup>, Olivier Dulieu<sup>2</sup>, Stefan Willitsch<sup>1</sup> \*

<sup>1</sup>University of Basel, <sup>2</sup>Laboratoire Aimé Cotton du CNRS, Orsay Cedex, France

We present extensions to our hybrid trap experiment with the aim to further increase the control over the chemical reactions we investigate. The hybrid trap consists of a linear Paul trap for the atomic and molecular ions and is overlapped with a magneto-optical trap for the neutral rubidium atoms. Initial experiments focused on the reactions between  $\text{Ca}^+ + \text{Rb}$  [1,2] and  $\text{Ba}^+ + \text{Rb}$  [3], in which both systems have been laser cooled. Additionally, reactions of sympathetically cooled  $\text{N}_2^+$  molecular ions with Rb atoms have been studied as well [4].

So far, the ability to precisely control the collision energy of the ion-atom system was limited. Different collision energies were accomplished by varying the amount of ions, which lead to large spreads of the collision energy for large ion numbers. In an effort to increase our collision energy resolution, we modified the magneto-optical trap to allow the formation of a tunable moving trap. The moving trap is achieved by using radiation pressure differences in the cooling laser beams and on-resonance push beams. By carefully tuning the cooling and push beam sequence and intensities we are able to produce moving atom clouds of well-defined velocities in the lab-frame. Using these moving atom clouds together with small ion numbers greatly improves our collision energy resolution.

For the ions, using sympathetically cooled, vibrationally state-selected  $\text{O}_2^+$  molecular ions enables the study of the role of vibration on reactive collisions. This will give us new insight into the dynamics of cold ion-neutral chemistry.

[1] Felix H.J. Hall et al; *Phys. Rev. Lett.* **2011** 107, 243202.

[2] Felix H.J. Hall, Pascal Eberle et al; *Mol. Phys.* **2013**, 111, 14-15, 2020-2032.

[3] Felix H.J. Hall et al; *Mol. Phys.* **2013**, 111, 12-13, 1683-1690.

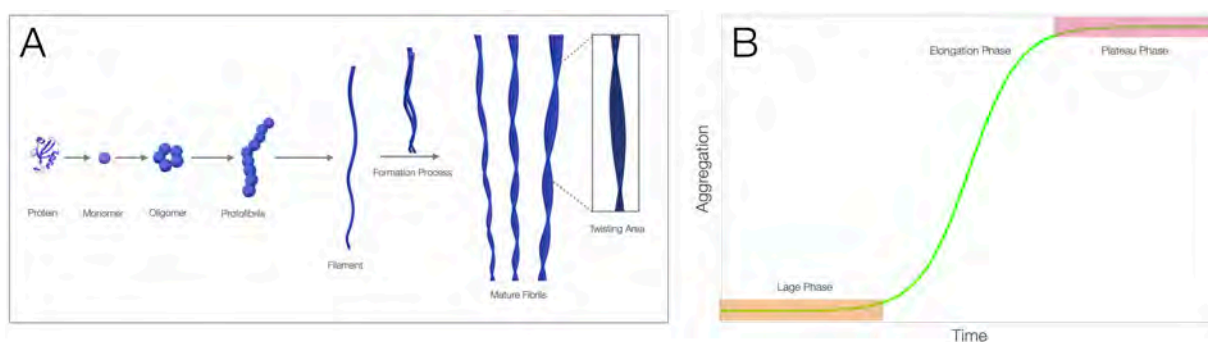
[4] Felix H.J. Hall et al; *Phys. Rev. Lett.* **2012** 109, 233202.

## Photo-induced fibril formation

Lukas Frey<sup>1</sup>, Peter Hamm<sup>1</sup> \*

<sup>1</sup>University of Zurich

The accumulation of abnormally folded proteins or peptides are associated with human neurodegenerative disorders. Overall 25 amyloid forming proteins in the human genome have been linked to severe neurodegenerative diseases [1]. Therefore, the understanding of amyloid fibril formation is very important for understanding these diseases for a better cure. In general the fibril formation process can be characterized in three phases: the lag, elongation and plateau phase (Fig. 1B, [2]). The process is initiated by a partially unfolded protein with high aggregating tendency (monomer, Fig. 1A). The aggregation of the monomers leads to different intermediates (oligomers, protofibrils, filaments, Fig. 1A, [2]) of the fibril formation process during the elongation phase. Entwining of filaments leads to mature fibrils with characteristic twisting areas. But the major problem in the investigation of the fibril formation process is the length of the lag phase, which is difficult to regulate because it depends on pH, temperature, concentration of the fibril evolving species and other parameters of the environment. A photo-induced fibril formation would generate a lag phase of equal length [3].



Here we present a PDZ2 domain from human tyrosine-phosphatase 1E (hPTP1E), where the fibril formation process can be controlled by radiation by attaching a covalently linked azobenzene alongside the binding groove of the PDZ 2 domain [4]. UV-Vis radiation induces a *trans-cis*-isomerisation of the azobenzene, which leads to a conformational change in the protein and to an aggregation process. The aggregation process leads to the formation of oligomers, protofibrils and mature fibrils. Further structural change in fibrils depending as a function of the radiation intensity was monitored. We conclude that the photo-induced fibril formation is an excellent system for studying the fibril formation process.

[1] David Eisenberg, *Cell*, **2012**, 148, 1188-1203

[2] Jan Bieschke, *Nature Chemical Biology*, **2012**, 8, 93-101

[3] Todd M. Doran, *ACS Chem. Neurosci.*, **2012**, 3, 211-220

[4] Brigitte Buchli, *PNAS*, **2013**, 110, 11725-11730

**Photprotection of an oxazine dye by quencher amino acids in model peptides**

Alexandre Fürstenberg<sup>1</sup>, Mélanie Villard<sup>1</sup>, Marianne Paolini-Bertrand<sup>1</sup>, Oliver Hartley<sup>1</sup>, Thomas Huber<sup>2</sup>, Thomas P. Sakmar<sup>2</sup>

<sup>1</sup>University of Geneva, <sup>2</sup>The Rockefeller University

Advanced fluorescence microscopy techniques including single-molecule and super-resolution imaging require bright and photostable fluorophores that can be selectively targeted to biomolecules, in particular to proteins. Proteins may contain however amino acids such as tryptophan and tyrosine which may quench nearby fluorophores by photoinduced electron transfer (PET). PET between fluorophores and amino acids is usually investigated by mixing the free components in aqueous solution and varying the quencher (amino acid) concentration. Such experiments however do not reflect the real situation where exactly one dye molecule is quenched by exactly one amino acid within a given protein. We therefore labeled model peptides of controlled amino acid sequence with the fluorophore ATTO655, an oxazine dye widely used in single-molecule imaging, and studied the influence of the peptide sequence on the fluorescence quantum yield of the dye and on its photostability. We confirmed that tryptophan and tyrosin quench ATTO655 both free in solution and within model peptides mainly due to static quenching and found that PET between the dye and quencher amino acids had a photoprotective effect on the dye, both in bulk solution and in single-molecule measurements on a glass surface. This suggests that PET can be used as a photoprotection mechanism in single-molecule experiments.

## Observation and theory of electric-dipole-forbidden infrared transitions in cold molecular ions

Matthias Germann<sup>1</sup>, Xin Tong<sup>1</sup>, Stefan Willitsch<sup>1</sup> \*

<sup>1</sup>University of Basel

Homonuclear diatomic molecules do not show a rotational-vibrational spectrum within the electric-dipole approximation. However, higher order terms in the multipole-expansion of their charge distribution give rise to weak lines in their rovibrational spectrum, so called dipole-forbidden transitions.

For molecular ions, the low intensity of these transitions has so far precluded their detection. Here we report the – to our knowledge – first observation of such transitions in molecular ions. More specifically, we have observed electric-quadrupole infrared fundamental transitions in  $\text{N}_2^+$  ions. For these observations the ions were produced in a selected internal quantum state, sympathetically cooled to millikelvin temperatures and stored in a linear Paul trap [1, 2]. The ions were vibrationally excited with a quantum cascade laser and the excitation was detected using a state-selective charge transfer reaction with argon atoms [3] that allows us to monitor absorption events on the single-molecule level. To understand the measured spectra, we have also developed the theory of hyperfine-resolved quadrupole infrared transitions in Hund's case b molecules.

The weakness of these dipole-forbidden transitions is associated with an extremely narrow linewidth. Thus their observation may open up new applications in precision spectroscopy such as the investigation of possible variations of fundamental constants [4].

[1] X. Tong, A. H. Winney, and S. Willitsch, *Phys. Rev. Lett.*, **2010**, 150, 143001

[2] X. Tong, D. Wild, and S. Willitsch, *Phys. Rev. A*, **2011**, 83, 023415

[3] S. Schlemmer, et al., *Int. J. Mass Spectrom.*, **1999**, 185, 589-602

[4] M. Kajita, et al., *Phys. Rev. A*, **2014**, 89, 032509.

## Nanoparticle - polyelectrolyte composites investigated by ATR-IR spectroscopy: Enhanced IR absorption and electron transfer upon visible light illumination

Harekrishna Ghosh<sup>1</sup>

<sup>1</sup>University of Geneva

Attenuated total reflection infrared (ATR-IR) spectroscopy is used to study the formation and the properties of nanoparticle-polyelectrolyte composites on a Ge internal reflection element. First the Ge ATR crystal is functional-ized using plasma cleaning and positively charged polyelectrolyte poly (al-lylamine hydrochloride) (PAH). Then citrate-stabilized nanoparticles are ad-sorbed onto the modified Ge ATR crystal. The layer-by-layer growth of polyelectrolytes (PAH and PSS; poly (sodium 4-styrenesulfonate)) on top of the nanoparticles is followed in situ. Enhancement of polyelectrolyte signal is observed and is more pronounced very near to the nanoparticles surface (Fig. 1). Also, stronger enhancement is observed from bigger nanoparticles. Upon illumination of the sample with visible light (VL) a strong IR absorption is observed due to the holes in the valence band of Ge, which indicates electron transfer from the Ge to the gold nanoparticles (Fig. 2).

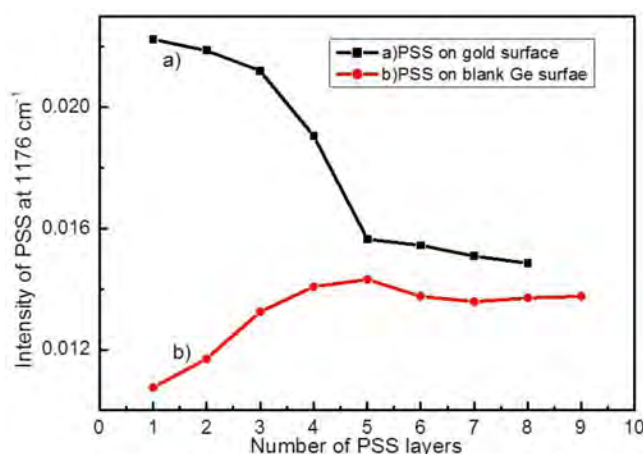


Fig.1. Enhancement of PSS signal from nanoparticle surface

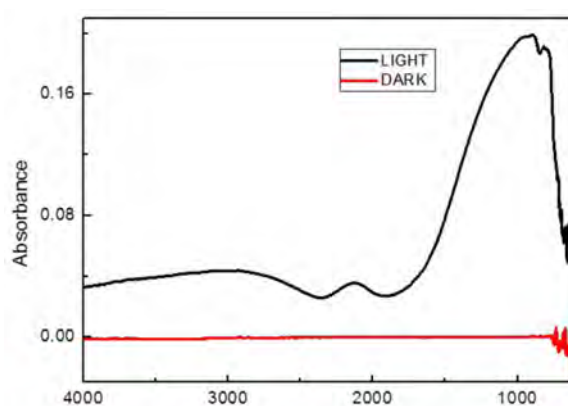


Fig.2. Strong IR absorption on GNP attached Ge surface upon VL illumination

- [1] T. Nagao, *et al.*, *Physical Chemistry Chemical Physics* **2011**, *13*, 4935.  
[2] P. D. Fairley, *et al.*; *J. Phys. D: Appl. Phys.* **2000**, *33*, 2837.

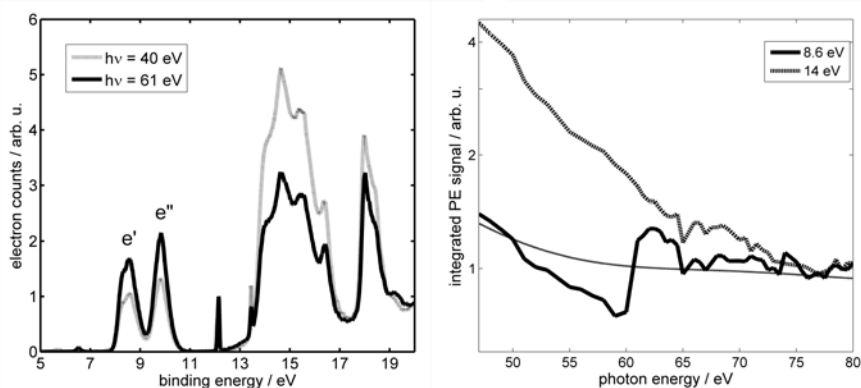
## Quantifying a Molecular Orbital's Character using Resonant Photoemission

Jakob Grilj<sup>1</sup>, Sistrunk Emily<sup>2</sup>, Brian McFarland<sup>3</sup>, Johan Rohlen<sup>4</sup>, Alejandro Aguilar<sup>5</sup>, Majed Chergui<sup>1</sup>, Markus Gühr<sup>2</sup> \*

<sup>1</sup>EPFL Lausanne, <sup>2</sup>Stanford University, <sup>3</sup>Los Alamos National Laboratory, <sup>4</sup>University of Gothenburg, <sup>5</sup>Lawrence Berkeley National Laboratory

Molecular orbitals are derived by mixing the constituents' atomic orbitals, a formalism known as linear combination of atomic orbitals (LCAO). Photoelectron spectroscopy (PES) is one of the few methods that can give quantitative, experimental values for orbital mixing. To this end, the photoelectron and Auger electron yield are measured as a function of photon energy and the line shape is analyzed using the so-called Fano formalism [1,2].

In this contribution, we present high resolution PES for iron pentacarbonyl, Fe(CO)<sub>5</sub>. We observe an interference at the resonance energy of the 3p-3d transitions of iron. We use the modulation depth of the Fano resonances to reinterpret the photoelectron lines in the literature. The resonance is also present in photolines attributed solely to the CO ligands.



Left: Photoelectron spectrum of Fe(CO)<sub>5</sub> at two incident photon energies showing resonant enhancement of certain photolines.

Right: The interference around 61 eV present in these photolines is a quantitative measure for the iron d orbital character of the molecular orbital in Fe(CO)<sub>5</sub>.

[1] E. Solomon, L. Basumallick, P. Chen, P. Kennepohl, P. *Coord. Chem. Rev.* **2005**, 249, 229; J. Green, P. Declava, *Coord. Chem. Rev.* **2005**, 249, 209

[2] U. Fano, J. Cooper, *Rev. Mod. Phys.* **1968**, 40, 441; L. Davis, L. Feldkamp, *Phys. Rev. B* **1981**, 23, 6239

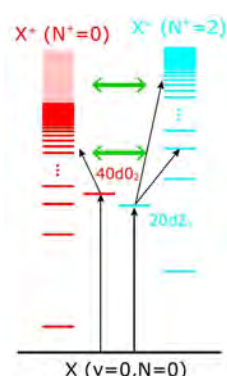
[3] E. Sistrunk, J. Grilj, B. McFarland, J. Rohlén, A. Aguilar, M. Gühr, *J. Chem. Phys.* **2013**, 139, 164318

## First rotational interval of para $\text{H}_2^+$ by Rydberg spectroscopy of $\text{H}_2$ in the range of 0.3-7 THz

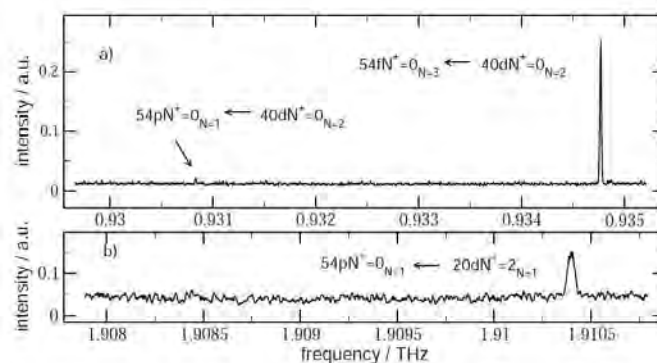
Christa Haase<sup>1</sup>, Maximilian Beyer<sup>1</sup>, Frédéric Merkt<sup>1</sup> \*

<sup>1</sup>Laboratory of Physical Chemistry, ETH Zurich, 8093 Zurich, Switzerland

$\text{H}_2^+$  does not have an electric dipole-allowed rotational or vibrational spectrum so that the rotational structure of the  $X^2\Sigma_g^+$  ( $v^+=0$ ) ground state has never been measured with high precision. We present here measurements of transitions between Rydberg states of para  $\text{H}_2^+$  converging to the  $N^+=0$  and  $N^+=2$  rotational levels of the  $X^2\Sigma_g^+$  ( $v^+=0$ ) ground state in the range of 0.3-7 THz. To access series converging on the  $N^+=0$  and  $N^+=2$  rotational thresholds from the same initial Rydberg level and to obtain an exact value for the energy difference between these thresholds we exploit the rotational channel interactions as depicted schematically in Fig 1.



Extrapolation of the series measured in the range of principal quantum number  $n=22-80$  by multichannel quantum defect theory enabled the determination of the  $N^+=0-N^+=2$  interval with unprecedented precision. The analysis of the spectra also provided information on the interactions between  $l=1$  (p) and  $l=3$  (f) ionization channels in para  $\text{H}_2$ . As an example, Fig 2a) and b) show transitions to the  $54pN^+=0_{N=1}$  and  $54fN^+=0_{N=3}$  levels recorded from  $40dN^+=0_{N=2}$  and  $20dN^+=2_{N=1}$  states, respectively.



## High-Resolution Absorption Spectroscopy in the Vacuum-Ultraviolet using Modulation Techniques

U. Hollenstein<sup>1</sup>, H. Schmutz<sup>1</sup>, Frédéric Merkt<sup>1</sup> \*

<sup>1</sup>Laboratory of Physical Chemistry, ETH Zurich, 8093 Zurich, Switzerland

High-resolution absorption spectroscopy in the vacuum ( $\lambda \leq 200\text{nm}$ ; VUV) and extreme ( $\lambda \leq 105\text{nm}$ ; XUV) ultraviolet ranges of the electromagnetic spectrum is notoriously difficult. VUV radiation from synchrotron sources needs to be monochromatised, which limits the bandwidth of the radiation to at best  $0.1\text{cm}^{-1}$  [1]. VUV-FT absorption spectroscopy, as recently extended to the XUV range offers the multiplex advantage, but so far the best resolution achieved with this method is  $0.33\text{cm}^{-1}$  [2]. Pulsed VUV laser systems based on four-wave mixing enable a higher resolution [3], but the large pulse-to-pulse fluctuations resulting from the non-linearity of the VUV generation process limits the sensitivity of absorption measurements, so that only very few laser VUV absorption spectra of atoms and molecules in supersonic beams have been reported [3, 4]. To improve the low sensitivity resulting from the large pulse-to-pulse fluctuation of the VUV radiation, Somnavilla et al. [5] have used a dispersion grating and exploited the beam diffraction in the negative first order to normalise the VUV laser intensity pulse by pulse and were able to reliably measure absorption signals of  $10^{-4}$ .

We present here an alternative method to record absorption spectra with high sensitivity that relies on frequency modulation techniques. The VUV radiation is produced by two-photon resonance-enhanced ( $\nu_{\text{VUV}} = 2\nu_1 \pm \nu_2$ ) four-wave mixing in Kr using the  $^1S_0 \rightarrow 4p^5 5p[1/2]$  ( $J = 0$ ) resonance at  $2\nu_1 = 94092.96\text{cm}^{-1}$  using the output of two FT-limited pulsed lasers (pulse length 5ns, obtained by pulse amplification of cw ring laser radiation). The modulation of the VUV laser frequency is achieved by generating side bands on the output of the second laser ( $\nu_2$ ) using an electro optical modulator. These side bands are automatically transferred to the VUV because the four-wave mixing process is linearly dependent on the intensity of the second laser. The poster will present numerical simulations of absorption experiments with this new method in model systems using parameters corresponding to experiments with supersonic beams. The simulations will be compared with experimental results.

[1] Laurent Nahon, Christian Alcaraz, Jean-Louis Marlats, Bruno Lagarde, François Polack, Roland Thissen, Didier Lepère and Kenji Ito, *Rev. Sci. Instr.* **72**, 1320 (2001).

[2] N. de Oliveira, D. Joyeux, D. Phalippou, J. C. Rodier, F. Polack, M. Vervloet and L. Nahon, *Rev. Sci. Instr.* **80**, 043101 (2009).

[3] P. C. Hinnen, S. Stolte, W. Hogervorst and W. Ubachs, *J. Opt. Soc. Am. B* **15**, 2620 (1998).

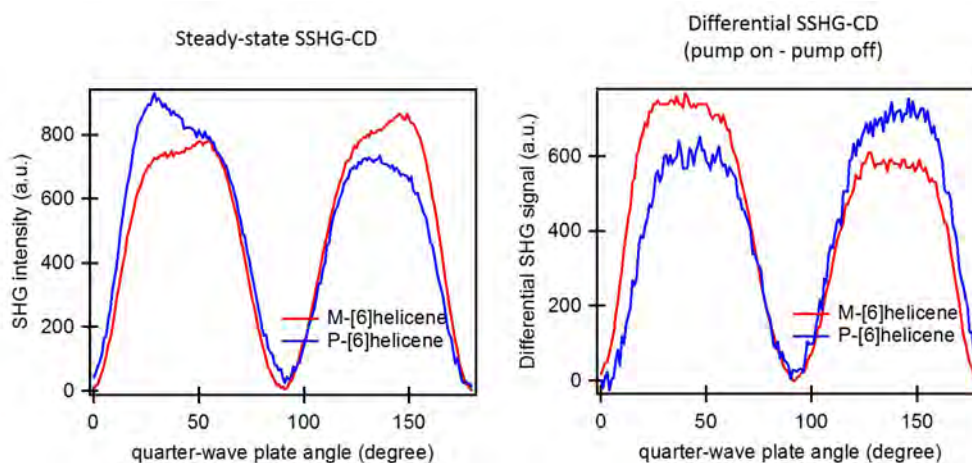
[4] T. P. Softley, W. E. Ernst, L. M. Tashiro and R. N. Zare, *Chem. Phys.* **116**, 299 (1987).

[5] M. Somnavilla, U. Hollenstein, G. M. Greetham and F. Merkt, *J. Phys. B: At. Mol. Opt. Phys.* **35**, 3901 (2002).

**Excited-state dynamics of chiral molecules at the liquid-liquid interface**Cho-Shuen Hsieh<sup>1</sup>, Johann Bosson<sup>1</sup>, Jérôme Lacour<sup>1</sup>, Eric Vauthey<sup>1</sup> \*<sup>1</sup>University of Geneva

Chiral molecules are present in various biological systems and the chirality differently affects their functionality. Surface second-harmonic-generation with circular dichroism (SSHG-CD) spectroscopy has been widely used to investigate the conformation of these interfacial chiral molecules due to its surface-specificity unlike standard CD spectroscopy [1,2]. The two enantiomers, which are mirror images of each other, have equal amplitude with opposite sign of the magnetic dipole moments, therefore leading to the different responses for the left- and right-hand circularly polarized light in the SSHG-CD spectroscopy (left panel). Combination of the SSHG-CD spectroscopy and the pump-probe technique allows us to probe the structural and population dynamics of these molecules.

In this presentation we will introduce the time-resolved (TR)-SSHG-CD technique. By exciting the [6]helicenes to the electronically excited state, we study the conformation and population dynamics of this chiral molecule at the dodecane-water interface. The left panel shows the steady state SSHG-CD intensity versus the angle between the fast axis of the quarter-wave plate and the axis of p-polarized fundamental light incident on the wave plate. Repeating the same measurement but 3 ps after optical excitation of the helicene to the lowest singlet excited state gives a different signal. The right panel shows the difference between the SSHG signals recorded with and without optical excitation. The two panels show opposite trend, which indicates that, upon excitation, the chirality of the molecules decreases. This may result from the structural changes in the excited state. Our data demonstrate that with this TR-SSHG-CD technique, it is possible to determine the time scale of the change in chirality and population from the excited to the ground state.



[1] Byers, J. D.; Yee, H. I.; Hicks, J. M. *J. Chem. Phys.* **1994**, *101*, 6233.

[2] Persechini, L.; McGilp, J. F. *Phys. Status Solidi* **2012**, *249*, 1155-1159.

## Mass Accommodation Coefficients and Evaporation Rates of H<sub>2</sub>O, HCl and HNO<sub>3</sub> on Atmospheric Ices in the Range 170 to 210 K.

Riccardo Iannarelli<sup>1</sup>, Michel J. Rossi<sup>1</sup> \*

<sup>1</sup>Paul Scherrer Institute, Villigen

The persistence or evaporative life time of Cirrus clouds in the Upper Troposphere and/or or Polar Stratospheric Clouds (PSC's) in the Lower Stratosphere depends on the partial pressure of H<sub>2</sub>O vapor, on atmospheric trace gases (HCl, HNO<sub>3</sub>) as well as on kinetic parameters such as the mass accommodation coefficients and evaporation rates at low temperatures. Using a kinetic stirred-flow reactor (SFR) [1] with a gas life time of several to several tens of seconds we have been able to measure the uptake and evaporation kinetics of atmospheric gases on thin deposited micron-size ice films as proxies of atmospheric ice particles and confirm and/or extend known phase diagrams of HCl and HNO<sub>3</sub> hydrates [2]. The SFR was configured as a multidagnostic experiment probing the gas- and condensed phase simultaneously using residual gas mass spectrometry, total pressure measurements and FTIR absorption spectroscopy in transmission.

The enclosed Figure displays example data on the thermodynamically stable form of nitric acid trihydrate, HNO<sub>3</sub>·3H<sub>2</sub>O or beta-NAT. We will present representative kinetic results on thin crystalline films of HCl·6H<sub>2</sub>O, amorphous H<sub>2</sub>O/HCl mixtures as well as on alpha- and beta NAT and metastable nitric acid dihydrate, NAD or HNO<sub>3</sub>·2H<sub>2</sub>O. The ratio of the mass accommodation coefficient and the rate of evaporation yields the equilibrium vapor pressure of H<sub>2</sub>O, HCl and HNO<sub>3</sub> which will be compared to the corresponding vapor pressures known from published phase diagrams. One of the main conclusions from the kinetic investigations is the fact that the rate of evaporation of the contaminants (HCl, HNO<sub>3</sub>) is always lower than for H<sub>2</sub>O which means that once contaminated, atmospheric ice remains so until complete evaporation of the contaminated ice particle. This has consequences for the chemical reactivity of contaminated ice particles in the atmosphere.

[1] Simone Chiesa, Michel J. Rossi, *Atmos. Chem. Phys.* **2013**, *48*, 11905-2013.

[2] Riccardo Iannarelli, Michel J. Rossi; *Atmos. Chem. Phys. Discuss.* **2013**, *13*, 30765-30839.

## Exciplex Formation in Bimolecular Photoinduced Electron-Transfer Investigated by Ultrafast Time-Resolved Infrared Spectroscopy

Marius Koch<sup>1</sup>, Romain Letrun<sup>1</sup>, Eric Vauthey<sup>1</sup> \*

<sup>1</sup>University of Geneva

The availability of ultrafast spectroscopy has opened a powerful pathway to look in real-time at short-lived intermediates in electron transfer (ET) processes between donor (D) and acceptor (A) molecules. One intermediate of these photochemical processes can be an excited complex (exciplex) which is believed to influence charge separation and recombination in solution, as well as in organic semiconductors, DNA or the photosynthetic reaction center.

Usually its investigation is based on emission- and electronic spectroscopy, which are powerful, but have certain disadvantages e.g. broad and overlapping spectral bands or low oscillator strength due to their charge transfer character.

On the contrary, ultrafast time-resolved infrared spectroscopy (TRIR) can overcome these disadvantages but studies on exciplexes by means of this method are rare.

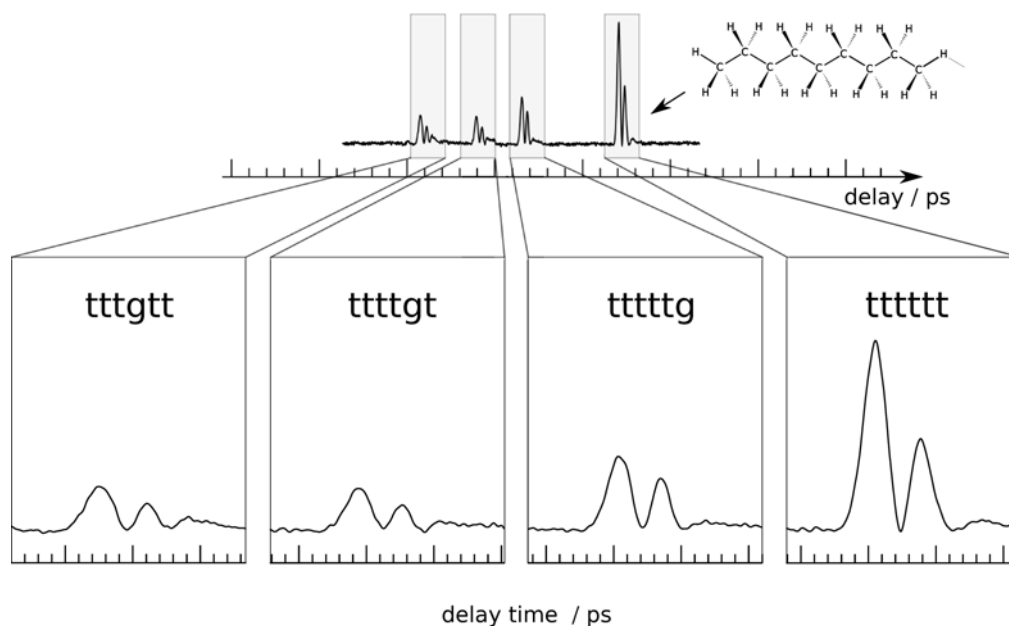
Using TRIR, we report on the observation of exciplexes formed between D/A pairs during bimolecular photoinduced ET in solution. The appearance of this and all other involved species in different frequency ranges and high signal intensity allows us to carry out a complete kinetic analysis without questionable assumptions. The analysis reveals that charge separation and recombination take place almost exclusively via the exciplex. Furthermore, the reconstruction of the anisotropy from polarization-resolved experiments supports a common rotation of D and A in the exciplex and uncovers their mutual orientation.<sup>[1]</sup>

In a continuative study on the dependence of driving force, solvent polarity and chemical structure of the exciplex constituents, we aim to demonstrate the general power of TRIR to understand how recombination is influenced if exciplexes are involved in photoinduced reactions.

[1] M. Koch, R. Letrun, E. Vauthey, *J. Am. Chem. Soc.* **2014**, *136*, 4066-4074.

**Accurate Structure of n-Nonane by Femtosecond Rotational Raman Spectroscopy**Philipp Kowalewski<sup>1</sup>, Hans-Martin Frey<sup>1</sup>, Samuel Leutwyler<sup>1</sup> \*<sup>1</sup>University of Berne

To obtain accurate rotational constants for the nonpolar molecule nonane ( $C_9H_{20}$ ) we used femtosecond time-resolved rotational Raman coherence spectroscopy. Due to the low vapor pressure of 3.8 mbar of nonane it is not possible to measure it in a gas cell experiment. By using a modified supersonic jet setup [1] we were able to determine the rotational constants of four different rotamers of n-Nonane, including the all-trans conformer.



[1] G. Brügger, H.-M. Frey, P. Steinegger, P. Kowalewski, *J. Phys. Chem. A*, **2011**, 115, 12380.

**Enhanced two-pulse orientation reveals anisotropy of molecular shape resonance**

Peter Kraus<sup>1</sup>, Denitsa Baykusheva<sup>1</sup>, Hans Jakob Wörner<sup>1</sup> \*

<sup>1</sup>ETH Zurich

We report the first experimental approach for generating field-free macroscopic orientation, i.e. 82% of a sample of CO molecules pointing in the same direction.

The achieved strong orientation enables us to reveal the spatial anisotropy of a molecular shape resonance in CO through high-harmonic spectroscopy. The resonance appears as a local maximum in the even-harmonic emission around 28 eV. In contrast, the odd-harmonic emission is suppressed in this spectral region. This surprising finding is explained by the phase anisotropy of the harmonic emission dipole between both recollision-sites, which causes a phase difference of exactly  $\pi$  at this particular photon energy through the combined effects of an asymmetric photorecombination phase and a sub-cycle Stark effect, generic for polar molecules. As high-harmonic spectroscopy of oriented molecules maps the sum (difference) of the electric fields emitted from both recollision-sites to the odd (even) harmonic orders, this phase difference causes destructive (constructive) interference for the odd (even) harmonic emission, respectively. The present study is to the best of our knowledge the first experimental demonstration of the anisotropy of a shape resonance in a polar molecule and the first experimental identification of the Stark phase contribution to high-harmonic generation.

The all-optical orientation scheme demonstrated in this study [1,2] relies on combining a one-color and a two-color non-resonant femtosecond laser pulse. It solely relies on the hyperpolarizability interaction as opposed to an ionization-depletion mechanism, which we show through quantitative modeling of the oriented rotational wave packet dynamics. The present orientation scheme opens a wide range of possible applications such as studies of attosecond charge migration, the recombination-site dependence of structural minima in photorecombination and side-dependent attosecond photorecombination delays.

[1] P. M. Kraus, D. Baykusheva, and H. J. Wörner, PRL, *under review*.

[2] P. M. Kraus, A. Rupenyan, and H.J. Wörner, PRL **109**, 233903 (2012).

**High-harmonic spectroscopy of attosecond charge migration in oriented molecules**

Peter Kraus<sup>1</sup>, Alisa Rupenyan<sup>1</sup>, Denitsa Baykusheva<sup>1</sup>, Johannes Schneider<sup>1</sup>, Hans Jakob Wörner<sup>1</sup>

\*

<sup>1</sup>ETH Zurich

A major goal of attosecond science is the real-time observation of electronic motion. Charge migration following ultrafast ionization has been predicted to occur on the femto- to attosecond time scales and to provide direct information on electron correlation in molecules.

In this contribution, we demonstrate the first application of high-harmonic spectroscopy to following attosecond correlation-driven charge migration in a molecule. We demonstrate our new methods on iodoacetylene (HCCI) because its cation displays configurational mixing between its two lowest electronic states. We impulsively orient the molecules using a recently developed all-optical scheme that enabled us to reach field-free molecular orientation. We then systematically measure the even and odd harmonics of aligned and/or oriented molecules using multiple wavelengths (0.8, 1.3 and 1.8  $\mu\text{m}$ ) and intensities. We further developed a new interferometric technique that allowed us to measure the phase of high-harmonic emission from aligned molecules using multiple wavelengths.

The combination of even and odd intensities with the phase measurements enables us to reconstruct attosecond charge migration in HCCI<sup>+</sup>. We measure that the hole takes 0.9 fs to move from one end of the molecule to the other and characterize the spatial evolution of the hole with an accuracy of  $\sim 100$  as. The comparison of our results with theory enables us to experimentally identify the importance of correlation-induced cross channels of HHG. These channels correspond to the electron tunneling from one and recombining to different single-electron orbitals, as a consequence of electron correlation. The observation of these channels also constitutes the first experimental evidence for electronic coherence in the cations using HHG.

Our results open the field of imaging the attosecond dynamics of charge-transfer phenomena in molecules.

**Sub-70 Femtoseconds Time-resolved Fluorescence Made Easy**Romain Letrun<sup>1</sup>, Eric Vauthey<sup>1</sup> \*<sup>1</sup>University of Geneva

Time-resolved fluorescence is an invaluable tool for the investigation of chemical, physical, and biological processes, as it allows monitoring the excited-state dynamics without contamination from that of other states. Several processes, such as excited-state proton transfer, electron transfer or the inertial component of solvent relaxation, can take place in a few tens or hundreds of femtoseconds,[1] pushing further the time resolution requirement. Femtosecond time resolution can be achieved by gating the fluorescence with an ultrashort laser pulse. Fluorescence up-conversion, one of the techniques based on this principle, is the most commonly used. In such an experiment, time resolution is, of course, mainly limited by the duration of the laser pulse, but also by three other factors: group-velocity dispersion (GVD), group-velocity mismatch (GVM), and phase-front mismatch (PFM). GVM and PFM cannot be eliminated simultaneously and are therefore the most limiting factors when trying to achieve sub-100 fs time resolution. On the other hand, GVD can be eliminated by limiting the number of transmissive optics and compensating for the dispersion of materials. However, focalising reflective optics, like off-axis parabolic mirrors and spherical mirrors, are often tedious to align and/or require a vast amount of space.

In this contribution, we present a compact and user-friendly fluorescence up-conversion set-up with a time resolution better than 70 fs whose capabilities will be illustrated through several examples.

[1] Arnulf Rosspeintner, Bernhard Lang, Eric Vauthey, *Annu. Rev. Phys. Chem.* **2013**, 64, 247-271

## Nanostructured Metallic Aerogels: High Performance Electrocatalysts for Fuel Cell Reactions

Wei Liu<sup>1</sup>, Anne-Kristin Herrmann<sup>1</sup>, Danny Haubold<sup>1</sup>, Mehtap Oezaslan<sup>2</sup>, Thomas J. Schmidt<sup>2</sup>, Alexander Eychmüller<sup>1</sup>

<sup>1</sup>Technische Universität Dresden, Germany, <sup>2</sup>Paul Scherrer Institute, Villigen

Despite large efforts in academia and industry, the commercialization of fuel cells, e.g. polymer electrolyte fuel cells, still faces critical issues including high catalyst cost, insufficient catalytic activity, and low durability.<sup>1</sup> Unsupported metal aerogels shed some promising light on improving both the catalytic activity and the durability, benefiting from their high extended surface area, large porosity and supportless structure.<sup>2-4</sup> We present here a facile spontaneous gelation strategy for the synthesis of a series of metallic aerogels, such as cyclodextrin modified Pd aerogels and bare Pt<sub>n</sub>Pd<sub>100-n</sub> aerogels.<sup>2-4</sup> These aerogels have nanowire-like network morphology, with the diameter of the nanowire of several nanometers. The aerogels have large porosity and very high surface area in the range of 70-170 m<sup>2</sup> g<sup>-1</sup>.<sup>2-4</sup> Electrochemical tests show that they have very high electrocatalytic activities combined with good durability towards ethanol oxidation or oxygen reduction reaction (ORR). For instance, the  $\beta$ -cyclodextrin modified Pd aerogels show a 2.3 times higher mass activity towards ethanol electrooxidation compared to that of the commercial Pd/C catalyst;<sup>2</sup> and the Pt<sub>80</sub>Pd<sub>20</sub> aerogels show a five times mass activity enhancement towards the ORR compared to that of the commercial Pt/C catalyst.<sup>3,4</sup> Furthermore, we present a newly developed strategy to design metal aerogels with nanotubular network structure. PtAg nanotubular aerogels with hierarchical porous structure and high surface area have been synthesized. The unique structure endows these aerogels with both excellent electrocatalytic activities toward formic acid oxidation (mass current density about seven times higher than that obtained from the commercial Pt black) and good electrochemical and structural durabilities. Our results show that metallic aerogels are a new class of promising fuel cell electrocatalysts. They may also find applications in other energy systems and catalysis.



[1] M. K. Debe, *Nature*, **2012**, 486, 43–51.

[2] W. Liu, et al., *Angew. Chem. Int. Ed.* **2012**, 51, 5743-5747.

[3] W. Liu, et al., *Angew. Chem. Int. Ed.* **2013**, 52, 9849–985.

[4] T. J. Schmidt, et al.; *European Patent Application* **2012**, EP 12177908.

**Pressure induced transformations in molecular crystals**

Piero Macchi<sup>1</sup>, Casati Nicola<sup>2</sup>

<sup>1</sup>University of Berne, <sup>2</sup>SLS, PSI Villigen

By applying pressure to solids, it is possible to obtain phase changes that stabilize molecular conformations or electronic configurations otherwise impossible to observe. Even more, chemical reactions could be induced, if the pressure is sufficiently large ( 20 GPa).

Some examples will be illustrated: a) proton transfer occurring in strongly hydrogen bonded carboxylic acids; b) nucleophilic additions of molecular crystals producing polymers, metastable at ambient conditions but stabilized at high pressure; c) rupture of aromaticity in annulene systems, leading more reactive species; d) breathing effects in metal organic frameworks.

All these important observations are obtained by measuring X-ray (or neutron) diffraction on single crystals or powder, inserted in diamond anvil cells. Experimental results are supported by theoretical predictions using periodic density functional theory.



**A Jet-CRDS Investigation of the  $\nu_2+2\nu_3$  band of  $^{13}\text{CH}_4$** Carine Manca Tanner<sup>1</sup>, Zoran Bjelobrk<sup>1</sup>, Martin Quack<sup>1</sup> \*<sup>1</sup>Laboratory of Physical Chemistry, ETH Zurich, 8093 Zurich, Switzerland

Methane is one of the most important molecular species in many areas, including applications in atmospheric chemistry, combustion science, planetary and space science. Hence the knowledge of its high resolution spectrum is necessary. While the main isotopomer  $^{12}\text{CH}_4$  has been subject to substantial spectroscopic efforts including recent analysis up to  $4700\text{ cm}^{-1}$  [1] and partial analysis up to  $6250\text{ cm}^{-1}$  [2], much less is known about the spectra of the second most important isotopomer  $^{13}\text{CH}_4$  with about 1% natural abundance, for which detailed systematic analyses have just started at the lower frequencies in our laboratory [3].

We have investigated the  $\nu_2+2\nu_3$  combination band of methane  $^{13}\text{CH}_4$  centered at  $7493.15918\text{ cm}^{-1}$ , the corresponding band system has been studied before for  $^{12}\text{CH}_4$  [4,5]. The jet-CRDS setup combining pulsed supersonic jet expansions and cavity ring-down spectroscopy (CRDS), which was already used for  $^{12}\text{CH}_4$  [5] and  $\text{H}_2\text{O}$  [6] has been used to record spectra of the Q and R branches at room temperature as well as at very low temperatures (down to 4 K). Based on our previous temperature-dependent investigations, we provide a careful analysis and an assignment for lines involving angular momentum quantum numbers up to  $J=4$ . The analysis of relative intensities in spectra taken at various rotational and effective translational temperatures indicates conservation of nuclear spin symmetry upon supersonic jet expansion, similar to the results for the main isotopomer [5].

Our work is supported by ETH, SNF and an ERC Advanced Grant.b

[1] S. Albert, S. Bauerecker, V. Boudon, L. R. Brown, J. P. Champion, M. Loete, A. Nikitin, M. Quack, *Chem. Phys.*, **2009**, 356, 131; S. Albert, K. Keppler Albert, M. Quack, High-resolution Fourier Transform Infrared Spectroscopy, in *Handbook of high-resolution spectroscopy*, edited by M. Quack and F. Merkt, Wiley, Chichester UK, **2011**, Vol. 2, pp. 965-1019.

[2] A. V. Nikitin, V. Boudon, L. R. Wenger, C. and L. Brown, S. Bauerecker, S. Albert, M. Quack, *Phys. Chem. Chem. Phys.*, **2013**, 15, 10071.

[3] H. M. Niederer, S. Albert, S. Bauerecker, V. Boudon, J. P. Champion, M. Quack, *Chimia*, **2008**, 62, 273; H. M. Niederer, X.-G. Wang, T. Carrington Jr, S. Albert, S. Bauerecker, V. Boudon, M. Quack, *J. Mol. Spectrosc.*, **2013**, 291, 33.

[4] M. Hippler, M. Quack, *J. Chem. Phys.*, **2002**, 116, 6045.

[5] C. Manca Tanner, M. Quack, *Mol. Phys.*, **2012**, 110, 2111.

[6] C. Manca Tanner, M. Quack, D. Schmidiger, *J. Phys. Chem. A*, **2013**, 117, 10105.

## Rational design of technical dawsonite-based sorbents for post-combustion CO<sub>2</sub> capture

Oliver Martin<sup>1</sup>, Markus Hammes<sup>1</sup>, Sharon Mitchell<sup>1</sup>, Javier Pérez-Ramírez<sup>1</sup> \*

<sup>1</sup>ETH Zurich

Among prospective post-combustion CO<sub>2</sub> capture sorbents, systems based on the formation of dawsonite (XAlCO<sub>3</sub>(OH)<sub>2</sub>, X = Na, K) have received limited attention, despite displaying attractive reversible uptakes under hydrothermal conditions.<sup>1,2</sup> Here, we combine understanding of the nanostructural transformations which originate the superior capacity of potassium dawsonite with respect to sodium dawsonite or hydrotalcite-based systems, with the mesoscale challenges faced in translating this promising performance to industrially-relevant forms (Fig. 1). In comparison with the extrusion of bulk precursors, the impregnation of alumina extrudates uniquely enables the attainment of shaped sorbents of non-negligible porosity and of variable potassium loading and distribution. Examination of internal sorbent cross-sections by scanning electron microscopy coupled with energy dispersive X-ray analysis and focused ion beam cutting clearly discerns the critical relation between these parameters and the loss of mechanical integrity due to internal stresses caused by the growth of needle-like dawsonite crystals upon carbonation. The latter can be avoided through the strategic application of common pore formers and binders, without compromising the net capacity, while favorably reducing kinetic limitations observed over densely-packed extrudates.

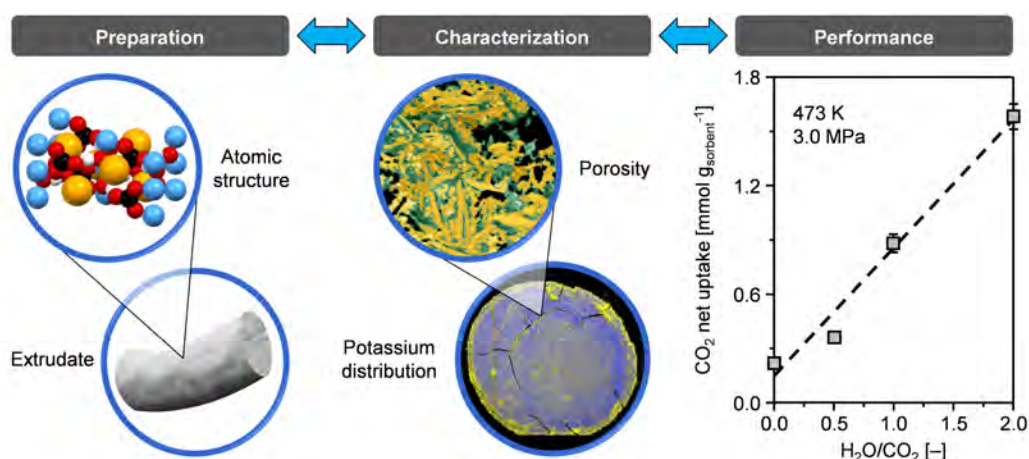


**Figure 1.** Multiscale aspects of rationalizing the design of dawsonite-based sorbents in extrudate form.

1. G. Stoica, J.C. Groen, S. Abelló, R. Manchanda, J. Pérez-Ramírez, *Chem. Mater.* **2008**, 20, 3973.
2. S. Walspurger, P.D. Cobden, W.G. Haije, R. Westerwaal, G.D. Elzinga O.V. Safonova, *Eur. J. Inorg. Chem.* **2010**, 2461.

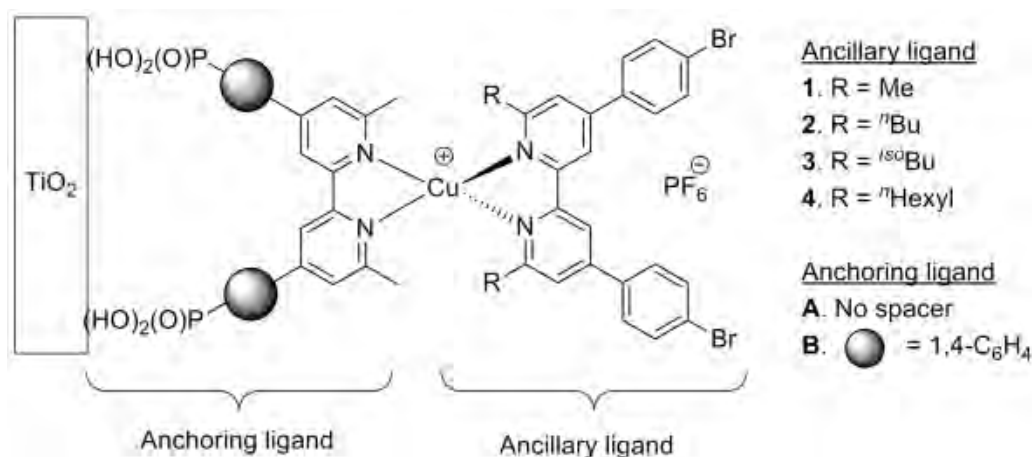
## Development of scanning electrochemical microscopy methods for the examination of copper(I) complexes in dye sensitized solar cells.

Colin Martin<sup>1</sup>, Catherine E. Housecroft<sup>1</sup>, Biljana Bozic-Weber<sup>1</sup>, Iain A. Wright<sup>1</sup>, Edwin C. Constable<sup>1</sup> \*

<sup>1</sup>University of Basel

The use of scanning electrochemical microscopy (SECM) as a tool to examine local electrochemical behavior in the solid state is becoming more common in modern material science.[1] Recent research within our group has focused upon the development of a number of novel dyes based on copper(I) coordination complexes with potential applications in dye sensitized solar cells (DSCs).[2] In order to assist with the development of devices and to better understand the processes resulting from changes in the cell setup, we have carried out preliminary investigations into the adaption of an SECM to examine the surface of DSCs both under illumination and in the dark. [3] Variations in both the complexes used as photosensitizer and the electrolytic system present in the cell have been studied with comparison of the surface currents observed giving information about both the solar cell topology and efficiency.

The examination of surface charges within dye sensitized solar cells (DSCs) containing copper(I)-based dyes has proved to be difficult due to the instability of these systems compared to existing commercial dyes. Here we report the use of SECM methodologies to investigate a series of  $[\text{Cu}(\text{L}_{\text{anchor}})(\text{L}_{\text{ancillary}})]^+$  sensitizers using homoleptic  $[\text{Cu}(\text{L}_{\text{ancillary}})_2]^+$  complexes as the active electrolyte, in which the ligands  $\text{L}_{\text{anchor}}$  and  $\text{L}_{\text{ancillary}}$  are 6,6'-disubstituted 2,2'-bipyridines (Figure 1). By using sensitizers and electrolytes containing the same ligands, changes in the diffusion layer around the scanning electrode have mapped the substrate surface both in the dark and under illumination. Examination of the changes in current as a constant potential is applied shows the formation of stable surface charge as the cell components equilibrate. Comparison of the time taken for this stabilization to occur as ancillary or anchoring ligands within the dye and electrolyte are varied shows a significant dependence upon the aliphatic substituents in the 6,6'-positions of the ligands which surround the copper(I) center.



[1] Bard, A. J.; Fan, F. R. F.; Kwak, J. and Lev O. *Anal. Chem.* **1989**, 61, 132-138.

[2] Bozic-Weber, B.; Brauchli, S.Y.; Constable, E.C.; Furer, S.O.; Housecroft, C.E.; Malzner, F.J.; Wright, I.A. and Zampese, J.A. *Dalton Trans.* **2013**, 42, 12293-12308.

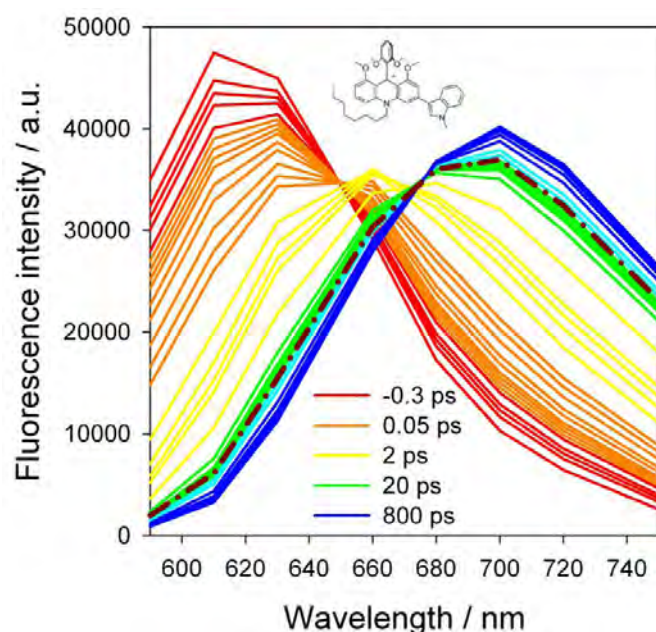
[3] Martin, C.J.; Bozic-Weber, B.; Constable, E.C.; Glatzel, T.; Housecroft C.E. and Wright I.A. *Electrochim. Acta.* **2014**, 119, 86-91.

**Ultrafast excited-state dynamics of new push-pull molecules**

Francois-Alexandre Miannay<sup>1</sup>, Rémi Vanel<sup>1</sup>, Alexandre Fürstenberg<sup>1</sup>, Jérôme Lacour<sup>1</sup>, Eric Vauthey<sup>1</sup> \*

<sup>1</sup>University of Geneva

Over the last decades, the need for new dyes for sensing biological environments has considerably increased. In this respect, push-pull dyes are particularly powerful probes and substantial effort is being invested in their design and synthesis. We will present new push-pull fluorescent probes, consisting of a positively charge pull moiety, an acridinium, linked to a indolic push group. We will show that the presence of the indol group confers to the molecule photophysical properties that differ substantially from those of the acridinium alone. chromophores, the acridiniums, have been synthesized adding some indolic group that give to the whole system some push-pull characteristics leading to amazing spectroscopic properties compared to simple acridinium system. Motivated by some former fluorescence imaging results in biological middle, we present here a set of steady-state and time-resolved spectroscopic results on indolyl-acridinium systems. Solvation studies and comparison between systems reveal that the early-time emission (0-1 ps after excitation) arising from some "simple acridinium specie" is then red-shifted at longer time scale. In parallel, while solvent polarity is decreasing, one time component of the fluorescence decay is increasing from 200 to 1300 ps, in acetonitrile and chlorophorm respectively. The same trend has been observed performing the time-resolved emission spectra in THF while increasing the electron donor properties of the indolic group. According to our results obtained at TCSPC, Fluorescence Up-conversion, and femtosecond visible transient absorption, this long time-component could be attributed to some possible charge transfer that occurred between the indole and the charge carbocation of the acridinium. This could be a first step in the explanation of the dye spectroscopic behavior in biological cells.



**Steps towards molecular parity violation: Population transfer experiments and absolute frequencies and quadrupole splittings of the lowest ro-vibrational levels ( $J=1$ ) of  $\nu_1$ ,  $\nu_3^{\pm 1}$ ,  $2\nu_4^0$  and  $2\nu_4^{\pm 2}$  in  $\text{NH}_3$**

Eduard Miloglyadov<sup>1</sup>, Peter Dietiker<sup>1</sup>, Andreas Schneider<sup>1</sup>, Georg Seyfang<sup>1</sup>, Martin Quack<sup>1</sup> \*

<sup>1</sup>ETH Zurich

According to ordinary quantum chemistry including only the electromagnetic interaction the ground state energies of enantiomers of chiral molecules are exactly equal by symmetry. However, this symmetry is broken by the electroweak interaction and a slight energy difference  $\Delta_{\text{PV}}E$  is introduced between the ground states of the two enantiomers [1-7], the measurement of which is the final goal of our study. The aim of the present work is to test both the population transfer efficiencies and the ultimate resolution of the setup for the parity violation experiment. As a test molecule the achiral molecule  $\text{NH}_3$  has been chosen. The molecule has large rotational constants and only the lowest rotational levels ( $J = 0,1$ ) are populated in a supersonic molecular beam. The absolute frequencies and quadrupole splittings of the ro-vibrational states of  $\nu_1$ ,  $\nu_3^{\pm 1}$ ,  $2\nu_4^0$  and  $2\nu_4^{\pm 2}$  have been measured in a pump-probe experiment. A ro-vibrational state has been populated through the absorption of an IR-photon from a continuous wave OPO locked to a frequency comb. In the second step molecules prepared in the excited ro-vibrational level have been probed selectively by a 2+1 REMPI process through the electronically excited B-state ( $E''$ ) or C-state ( $A_1'$ ). We report results on very efficient population transfer and very high resolution data including hyperfine splittings in  $^{14}\text{NH}_3$ . Acknowledgement: Our work is supported by an ERC Advanced Grant.

[1] M. Quack, *Chem. Phys. Lett.*, **1986**, 132, 147

[2] A. Bakasov, T.-K. Ha, M. Quack, *J. Chem. Phys.*, **1998**, 109, 7263

[3] R. Berger and M. Quack, *J. Chem. Phys.*, **2000**, 112, 3148

[4] M. Quack and J. Stohner, *Phys. Rev. Lett.*, **2000**, 84, 3807

[5] M. Quack and J. Stohner, *J. Chem. Phys.*, **2003**, 119, 11228

[6] M. Quack, J. Stohner, M. Willeke, *Annu. Rev. Phys. Chem.*, **2008**, 59, 741

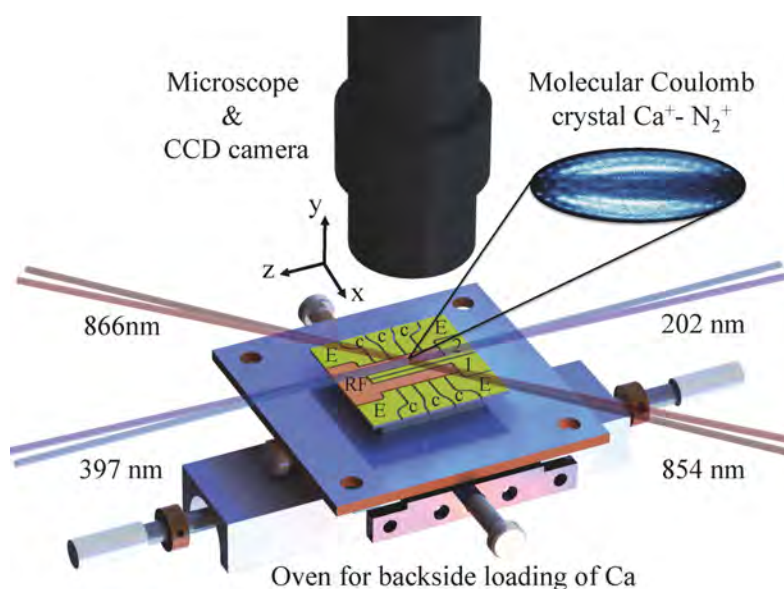
[7] M. Quack, 'Fundamental Symmetries and Symmetry Violations from High-resolution Spectroscopy', in Handbook of High-resolution Spectroscopy, Vol.1, pages 659 – 722, M.Quack and F.Merkt (eds.), Wiley, Chichester 2011

## Cold molecular ions on a chip

Arezoo Mokhberi<sup>1</sup>, Stefan Willitsch<sup>1</sup> \*

<sup>1</sup>University of Basel

Highly controllable cold molecular ions are of great interest for many applications in quantum information science, precision spectroscopy, cold chemistry and collision studies [1-3]. Molecular ions can be efficiently cooled sympathetically by the interaction with laser cooled, trapped atomic ions to form bi-component Coulomb crystals[4]. Surface-electrode radio frequency ion traps represent a new trapping architecture in which all electrodes lie in a plane and the ions are trapped above the surface [5,6]. This new generation of traps offer a high flexibility for manipulating, separating and shuttling of cold ions, which is relevant for, e. g., large-scale quantum information processing [5] and quantum optics experiments with trapped molecules [3]. We have developed a six-wire surface-electrode trap [7] with highly controllable trapping parameters to form planar [8] as well as spheroidal Coulomb crystals. Molecular ions have been trapped and sympathetically cooled in this device.



- [1] S. Willitsch, *Int. Rev. Phys. Chem.*, **2012**, 31 175-199.
- [2] J. Mur-Petit, et al., *Phys. Rev. A*, **2012**, 85, 022308.
- [3] D. I. Schuster, et al., *Phys. Rev. A*, **2011**, 83, 012311.
- [4] K. Mølhave and M. Drewsen, *Phys. Rev. A*, **2000**, 62, 011401.
- [5] J. Chiaverini, et al., *Quantum Inf. Comput.*, **2005**, 5, 419.
- [6] I. M. Georgescu, S. Willitsch, *Phys. Chem. Chem. Phys.*, **2011**, 13, 18852.
- [7] Allcock, D. T. C., et al., *New Journal of Physics*, **2010**, 12 (5), 053026.
- [8] I. Buluta and F. Nori, *Science*, **2009**, 326, 108-111.
- [9] R. Schmied, *New Journal of Physics*, **2010**, 12, 023038.

**Tryptophan-to-heme electron transfer in ferrous myoglobins**

Roberto Monni<sup>1</sup>, Andre Al Haddad<sup>1</sup>, Frank Van Mourik<sup>1</sup>, Gerald Auböck<sup>1</sup>, Majed Chergui<sup>1</sup> \*

<sup>1</sup>EPFL Lausanne

Tryptophan (Trp) is widely used in studies of protein dynamics based on Fluorescence Resonance Energy Transfer (FRET). In horse heart myoglobin (Mb) two tryptophan residues, Trp<sup>7</sup> and Trp<sup>14</sup> are located in the A-helix. It was long believed that both undergo FRET to the heme on timescales of 130 ps and 20 ps, respectively [1]. Recently, it was demonstrated that for ferric MetMb and its cyano-complex, Trp<sup>14</sup> relaxes predominantly via electron transfer (ET) to the heme [2], leading to a long-lived (lifetime 2 ns) reduced ferrous heme. Given the invariance of Trp lifetimes in all Mbs, it was suggested that an ET may also occur in ferrous Mbs [2]. This work explores the possibility of a Trp<sup>14</sup> to heme ET transfer in ferrous deoxy Mb. For this purpose, we compare visible probe transient absorption (TA) data for 290 nm (Trp and heme excitation) and 315 nm (only heme excitation) pump wavelengths. The results obtained by our experiments show that, upon 290 nm excitation, a transient signal with a lifetime 1 ns is observed which is not present upon 315 nm excitation. We identify this long lived state as a reduced heme porphyrin, which was previously never observed under physiological conditions. The reduction of Fe<sup>(III)</sup>-porphyrin complexes can lead either to the actual Fe<sup>(II)</sup> species or to the Fe<sup>(III)</sup>-porphyrin<sup>•-</sup> [3,4]. Comparing the absorption spectrum of our photoproduct to known spectra of formal Fe<sup>(II)</sup> porphyrins suggests that a photo-induced Trp<sup>14</sup> → heme electron transfer generates a Fe<sup>(III)</sup>-porphyrin radical anion.

[1] M. Hochstrasser and D. K. Negus, *Proc. Natl. Acad. Sci. U.S.A.* **1984**, 81, 4399.

[2] C. Consani, G. Auböck, F. Van Mourik and M. Chergui, *Science*, **2013**, 339, 1586.

[3] Donohoe, R.J., M. Atamian, and D.F. Bocian, *Journal of the American Chemical Society*, **1987**, 109, 5593.

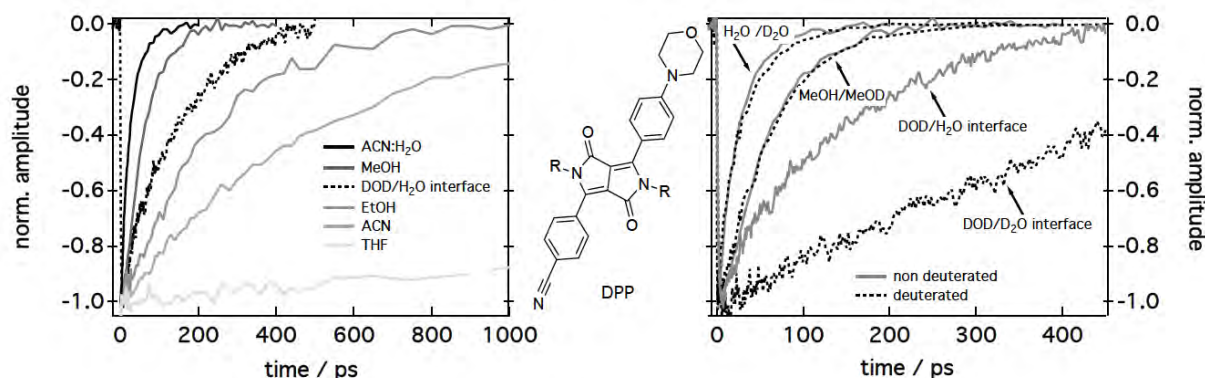
[4] Yamaguchi, K. and I. Morishima, *Inorganic Chemistry*, **1992**. 31, 3216.

## Excited-state dynamics of an environment-sensitive diketopyrrolopyrrole push-pull probe: major differences between the bulk solution phase and the dodecane/water interface

Sandra Mosquera Vazquez<sup>1</sup>, Sabine Richert<sup>1</sup>, Marek Grzybowski<sup>2</sup>, Daniel Gryko<sup>2</sup>, Alexander Kyrychenko<sup>3</sup>, Eric Vauthey<sup>1</sup> \*

<sup>1</sup>University of Geneva, <sup>2</sup>Polish Academy of Sciences, <sup>3</sup>V.N. Karazin Kharkiv National University

Liquid/water interfaces play a crucial role in many areas of science and technology. In organic synthesis, key chemical reactions involving water insoluble compounds have been found to be faster when in contact with water. To get a better understanding on how interfacial water affects the properties and reactivity of a solute molecule, we have compared the excited-state dynamics of a specially designed diketopyrrolopyrrole derivative (DPP) in bulk solution and at the dodecane/water interface, using a combination of ultrafast spectroscopic techniques, including time-resolved surface second-harmonic generation (TR-SSHG), complemented by molecular dynamic (MD) simulations. Bulk studies reveal that the excited-state dynamics of DPP is sensitive to the polarity and especially to the H-bond donor strength of the solvent. For example, the excited-state lifetime decreases from several nanoseconds in cyclohexane to 460 ps in acetonitrile and to less than 10 ps in water. At the dodecane/water interface, the excited-state lifetime is longer by a factor of ca. 20 than in water, and increases further by a factor of about 3 when going to the dodecane/deuterated-water interface. This isotope effect, that is more than twice as strong as that in solutions, as well as MD simulations indicate that the slowing down of the dynamics at the interface cannot be solely ascribed to a reduced accessibility of DPP to the aqueous phase. This slower excited-state decay is rather assigned to the conjunction of several effects, such as the strengthening of the H-bond network formed by the interfacial water molecules and the lower local polarity of the interfacial region. This investigation illustrates how photochemical reactivity can change by going from the bulk phase to an interface.



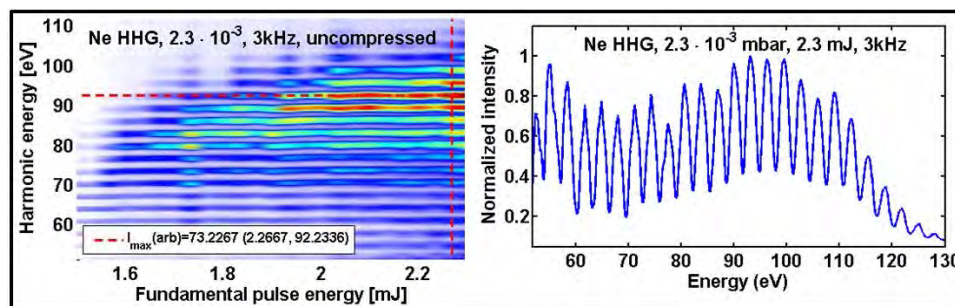
Ground-state recovery dynamics of DPP in solution and at the interface

## A table-top high-harmonic-generation-based source for valence/core level photoelectron spectroscopy in liquid samples.

Jose Ojeda<sup>1</sup>, Christopher Arrell<sup>1</sup>, Lars Mewes<sup>1</sup>, Haijuan Zhang<sup>1</sup>, Jakob Grilj<sup>1</sup>, Frank Van Mourik<sup>1</sup>, Majed Chergui<sup>1</sup> \*

<sup>1</sup>EPFL Lausanne

Many interesting dynamical processes in liquid solutions can be studied by means of time-resolved photoelectron spectroscopy [1]. Using high-harmonic generation (HHG), short high-energy photon pulses can be obtained, opening the possibility to study ultrafast dynamics in a compact table-top setup [2]. Various efficient configurations have been proposed for the HHG, depending on the desired photon energy [3,4]. However, these setups can be complex and/or have drawbacks in terms of repetition rate and maximum attainable photon energy. In our system we employ a Ti:Sapphire laser with tunable repetition rate (3-15 kHz), pulse duration (down to  $\approx 15$  fs with a gas-filled hollow-core fiber compressor) and average power (up to 15 W). In addition, we can tune the central wavelength of the fundamental by a small amount ( $\approx 15$  nm). Our experimental system allows a trade-off between the harmonic photon flux and the repetition rate, both having great influence on the signal-to-noise ratio of the photoelectron measurements. This simple setup, allows easily tuning and optimizing the energy range of the high harmonics in a few steps (see figure 1), thereby opening the possibility to continuously shift from valence to core-level sampling, with negligible interruption in the data acquisition process. To spectrally filter the harmonic energy, the incorporation of a time-preserving monochromator is being commissioned, with an expected transmission efficiency of about 10-20 % for the 10-100 eV photon energy range and a temporal resolution of about 30 (120) fs for the high (low) regimes of the same energy range [5].



- [1] H. Hüfner, Photoelectron spectroscopy: principles and applications, Springer (2003).  
 [2] O.Link, E. Vohringer-Martinez, E. Lugovoj, Y. Liu, K. Siefertmann, M. Faubel, H. Grubmüller, R. Benny-Gerber, Y. Miller and B. Abel, Ultrafast phase transitions in metastable water near liquid interfaces, Faraday Discussions, 141, 67–79 (2009).  
 [3] F. Brizuela, C.M. Heyl, P. Rudawski, D. Kroon, L. Rading, J.M. Dahlström, J. Mauritsson, P. Johnsson, C.L. Arnold and A. L’Huillier, Efficient highorder harmonic generation boosted by below-threshold harmonics, Scientific Reports, 3, 1410 (2013).  
 [4] Z. Chang, A. Rundquist, H. Wang, M.M. Murnane and H.C. Kapteyn, Generation of coherent soft X rays at 2.7 nm using high harmonics, Physical Review, 28, 2967–2970 (1997).  
 [5] F. Frassetto, C. Cacho, C.A. Froud, E. Turcu, P. Villorresi, W.A. Bryan, E. Springate and L. Poletto, Single-grating monochromator for extremeultraviolet ultrashort pulses, Optics Express, 19, 19169–19181 (2011).

## **Ultrafast spectroscopic investigation of carrier dynamics in Dye sensitized and perovskite based photovoltaics**

Arun Aby Paraecattil<sup>1</sup>, Jan C Brauer<sup>1</sup>, Arianna Marchioro<sup>1</sup>, Ahmad Ajdarzadeh<sup>1</sup>, Jacques-E. Moser<sup>1</sup>  
\*

<sup>1</sup>EPFL Lausanne

Interfacial electron transfer and carrier dynamics and related phenomena such as exciton formation, electron trapping etc. at femtosecond and picosecond timescales are of fundamental interest in the physics and chemistry of interfaces. Better understanding of these phenomena can contribute in the development of materials used in practical applications such as photovoltaics.

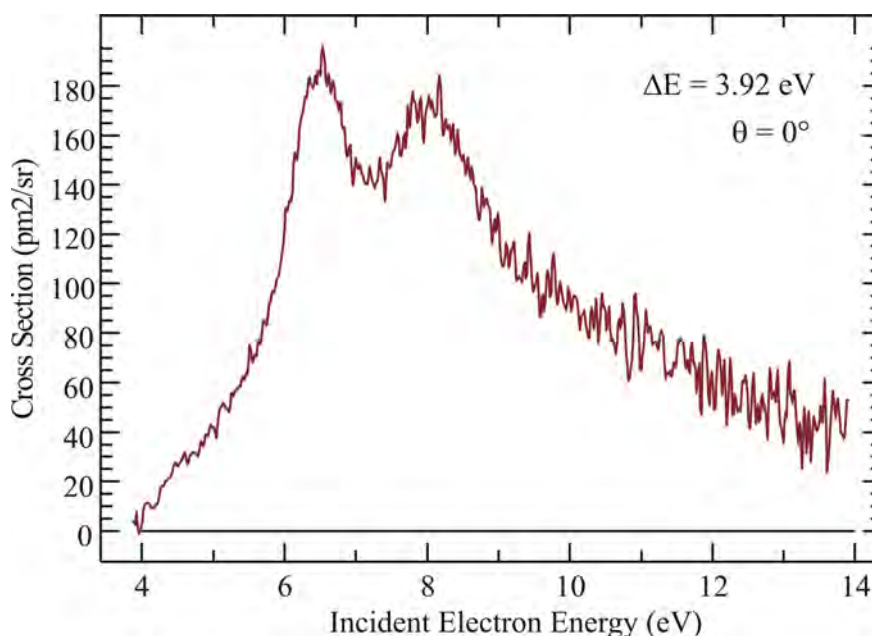
Using ultrafast pump-probe measurements, with probes in the visible as well as the THz regime we have demonstrated the formation of an intermediate charge transfer state at the Dye-TiO<sub>2</sub> interface. According to the current understanding of DSSCs functioning mechanism, charges are separated directly during this primary electron transfer process, yielding a hot conduction band electron in the solid and a positive hole localized on the oxidized dye molecule at the surface. Our finding founds a new mechanism for charge separation in Dye sensitized solar cells (DSSCs).

These techniques have also been applied to the investigation of perovskite-based photovoltaic devices. Spectroscopic investigations of charge carrier properties have been carried out to elucidate short and long-range carrier mobilities in the fs and ps time scales.

**Absolute cross sections of electronic excitation of furan**Khrystyna Regeta<sup>1</sup>, Michael Allan<sup>1</sup> \*<sup>1</sup>University of Fribourg

Electronic excitation plays a key role in FEBIP (focused electron beam induced processing) as the first step of neutral dissociation, an alternative to the much studied DEA (dissociative electron attachment). Furan was chosen as a model compound for a ligand in FEBIP precursors and because our study will test existing calculations [1-3]. Relative differential cross sections at 0° were already measured in our group [4].

We measured absolute differential cross sections (DCSs) for elastic scattering and for electronic excitation of furan and extended existing measurements [1-3] to the near-threshold region. Two resonances are observed in the excitation of the lowest triplet state (see Fig. 1) and we assign them as valence core excited resonances.



[1] R. F. da Costa, M. H. F. Bettega, M. A. P. Lima, M. C. P. Lopes, L. R. Hargreaves, G. Serna, and M. A. Khakoo, *Phys. Rev. A.*, **2012**, 85, 062706.

[2] J. B. Maljkovic, F. Blanco, R. Curik, G. Garcia, B. Marinkovic and A. Milosavljevic, *J. of Chem. Phys.*, **2012**, 137, 064312.

[3] M. H. Palmer, I. C. Walker, C. C. Ballard, M. F. Guest, *Chem. Phys.*, **1995**, 192, 111-125.

[4] K. Asmis, *PhD thesis, University of Fribourg, Switzerland*, **1996**.

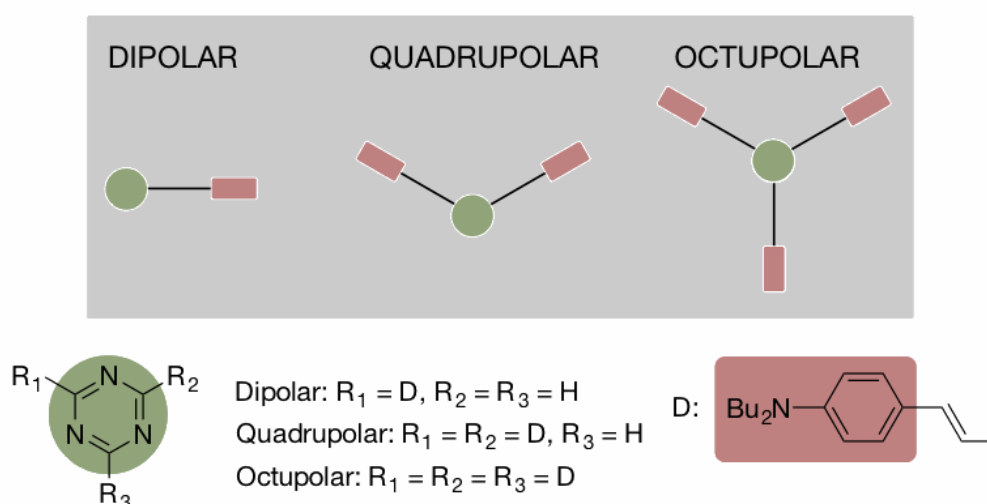
## Multibranching Effect of Dipolar Chromophores on (Non)Linear Photophysical Properties and Two-Photon Induced Polymerization

Arnulf Rosspeintner<sup>1</sup>, Julien Christmann<sup>1</sup>, Aleksandr Ovsianikov<sup>2</sup>, Aliasghar Ajami<sup>2</sup>, Max Tromayer<sup>2</sup>, Robert Liska<sup>2</sup>, Eric Vauthey<sup>1</sup> \*

<sup>1</sup>University of Geneva, <sup>2</sup>Vienna University of Technology

Two-Photon induced Polymerization (TPIP) is being heavily exploited in applications such as polymer-based optical waveguides on integrated circuit boards, or high-density 3D optical data storage.

In order to better understand the influence of molecular structure on both non-linear optical properties, such as two-photon absorption efficiency and the abilities to serve as photoinitiators, we have investigated a homologous series of three triazine-based model photoinitiators of dipolar, quadrupolar and octupolar nature. In particular, our investigation comprises the synthesis (including chemical characterization), photophysical characterization (including femtosecond transient absorption spectroscopy) and TPIP microstructuring tests.



We are confident, that our systematic interdisciplinary approach will allow to establish reliable structure-activity relationships for the development of future TPIP initiators.

## Observation of dipole-dipole and dipole-quadrupole interactions between pairs of ultracold cesium Rydberg atoms

Heiner Saßmannshausen<sup>1</sup>, Johannes Deiglmayr<sup>1</sup>, Hansjürg Schmutz<sup>1</sup>, Pierre Pillet<sup>2</sup>, Frédéric Merkt<sup>1</sup>\*

<sup>1</sup>Laboratory of Physical Chemistry, ETH Zurich, 8093 Zurich, Switzerland, <sup>2</sup>Laboratoire Aimé Cotton du CNRS, Orsay Cedex, France

We have used a pulse-amplified frequency-doubled ring dye laser with a 140 MHz Fourier-transform-limited bandwidth to excite ultracold cesium atoms to  $np_{3/2}$  Rydberg states with principal quantum numbers  $n$  between 22 and 180. We performed measurements at low ground-state atom density ( $\sim 10^9$  atoms/cm<sup>3</sup>) on atoms released from a magneto-optical trap and at increased density ( $\sim 10^{12}$  atoms/cm<sup>3</sup>) after loading the atoms in a crossed optical dipole trap. At low Rydberg atom density and after compensating electric and magnetic stray fields to  $\sim 1$  mV/cm and 2 mGs, respectively, millimetre-wave spectra of transitions between Rydberg states were recorded with a spectral resolution of 20 kHz [1].

At high densities, interactions between Rydberg atoms dominate the dynamics of the cold Rydberg gas, leading to effects such as e.g. the excitation blockade [2] in the case of excitation with narrow-band lasers and rapid many-body ionisation [3] in the case of pulsed broad-band excitation. We utilised the observed interaction-induced ionisation to detect Rydberg states with principal quantum number down to  $n = 22$  which cannot be directly field ionised in our setup. Under these conditions, and using laser intensities with which the atomic  $np_{3/2} \leftarrow 6s_{1/2}$  transitions are saturated, additional lines in the Rydberg spectrum were observed. By means of the scaling of their detuning from the corresponding  $np_{3/2}$  state with  $n$ , their Stark shift and calculations, we attribute these lines to  $ns_{1/2}-(n+1)s_{1/2}$  and  $ns_{1/2}-(n-3)f$  pair states (with  $n$  between 22 and 36). These pair states are dipole-dipole and dipole-quadrupole coupled (mixed), respectively, with corresponding  $np_{3/2}$ - $np_{3/2}$  states and are therefore accessible via two-photon transitions starting from a pair of cesium atoms in the  $6s_{1/2}$  electronic ground state.

Recently, we have installed an external enhancement cavity for continuous-wave (cw) frequency-doubling of the ring laser output. Up to 300 mW of cw UV radiation at wavelengths around 320 nm and a bandwidth of 1-2 MHz can be generated. This cw UV source can be used to study dipole-coupled Rydberg-atom pair states and to photoassociate cesium atoms to bound Rydberg-Rydberg molecules (so-called macrodimers [4]) in long-range potential wells that are predicted by our simulations.

[1] H. Saßmannshausen, F. Merkt, and J. Deiglmayr, Phys. Rev. A, **2013**, 87, 032519.

[2] D. Tong, S. M. Farooqi, J. Stanojevic, S. Krishnan, Y. P. Zhang, R. Côté, E. E. Eyler, and P. L. Gould, Phys. Rev. Lett., **2004**, 93, 063001.

[3] P. J. Tanner, J. Han, E. S. Shuman, and T.F. Gallagher, Phys. Rev. Lett., **2008**, 100, 043002.

[4] K. R. Overstreet, A. Schwettmann, J. Tallant, D. Booth, and J. P. Shaffer, Nature Physics, **2009**, 5, 581 - 585.

## Two-dimensional Raman-terahertz spectroscopy of water

Janne Savolainen<sup>1</sup>, Saima Nafees Ahmed<sup>1</sup>, Peter Hamm<sup>1</sup> \*

<sup>1</sup>University of Zurich

Although intermolecular solvent motions govern chemistry, the microscopic understanding of these bath interactions is still lacking. To that end, a novel two-dimensional Raman-terahertz (THz) spectroscopy is presented as a multidimensional spectroscopy directly in the far-IR regime [1-3]. The method is used to explore the dynamics of the collective intermolecular modes of liquid water at ambient temperatures that emerge from the hydrogen-bond networks water forms. Two-dimensional Raman-THz spectroscopy interrogates these modes twice and as such can elucidate couplings and inhomogeneities of the various degrees of freedoms. An echo in the 2D Raman-THz response is indeed identified, indicating that a heterogeneous distribution of hydrogen-bond networks exists, albeit only on a very short 100-fs timescale.

In extension to reference [1] we determined the response of a highly concentrated salt solution (3M NaCl). The inhomogeneity of the system is thus increased as some water molecules will occupy the solvation shells around the ions. This increase in the sample inhomogeneity is reflected clearly in the results as an extension of the lifetime and complexity of the diagonal echo feature (Figure 1). Some attention will also be paid to the technical details of the presented novel spectroscopy [4-5].

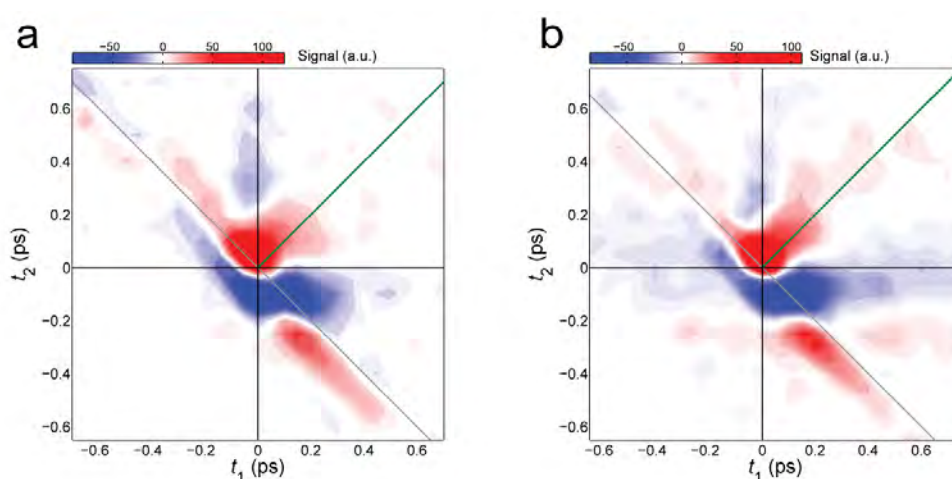


**Figure 1.** The 2D Raman-THz response of water (**a**) and 3M NaCl solution (**b**). The green lines indicate the diagonals ( $t_1=t_2$ ), along which the echoes are observed. The increased inhomogeneity of the 3M NaCl sample is seen as an increase in the lifetime and complexity of the diagonal feature.

[1] Janne Savolainen, Saima Ahmed, and Peter Hamm, PNAS, **2013**, 110, 20402.

[2] Peter Hamm, and Janne Savolainen, J. Chem. Phys., **2012**, 136, 094516.

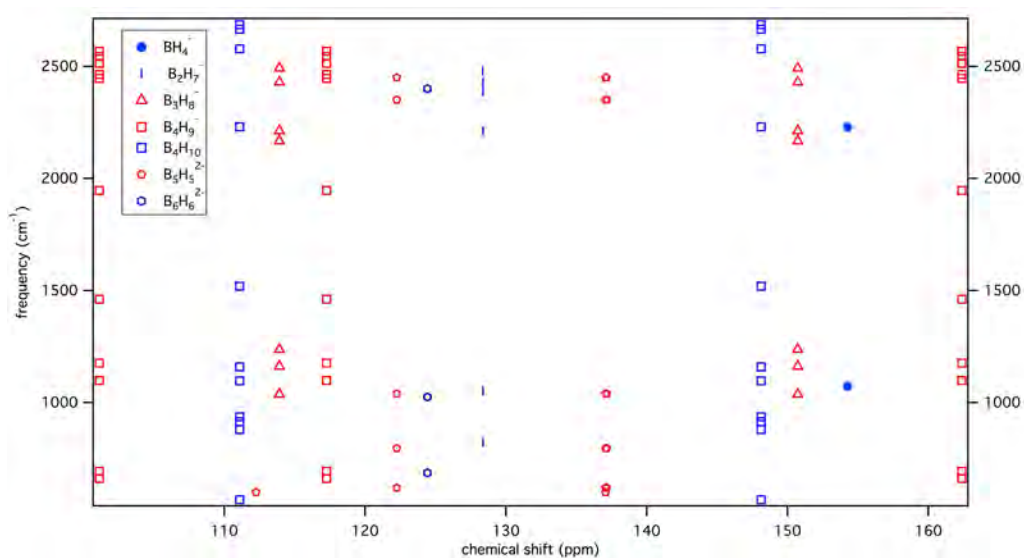
[3] Peter Hamm, Janne Savolainen, Junichi Ono and Yoshitaka Tanimura, J. Chem. Phys., **2012**, 136, 236101.

[4] Saima Ahmed, Janne Savolainen and Peter Hamm, Opt. Express., **2014**, 22, 4526.

[5] Saima Ahmed, Janne Savolainen and Peter Hamm, Rev. Sci. Inst., **2014**, 85, 013114.

**Computational Study of Spectroscopic Properties of Different Borohydride Species**Daniel Sethio<sup>1</sup>, Manish Sharma<sup>1</sup>, Hans Hagemann<sup>1</sup> \*<sup>1</sup>University of Geneva

Dehydrogenation of borohydrides is complex and pass through multistep processes<sup>1</sup>. There are several possible intermediates formed during decomposition processes<sup>2</sup>. Therefore the identification of intermediates is important. We studied  $B_xH_y$ ,  $H_xH_y^-$ ,  $B_xH_y^{2-}$  for  $x,y = 1-12$  species and predict the vibrational and NMR spectra using B3LYP/6-311++G\*\* level. The combination of vibrational and NMR spectra can help to identify the species observed, as vibrational or NMR spectra alone could lead to different candidates. The calculated spectra were compared with experimental data.



[1] M. Paskevicius, et.al., J. Phys. Chem. C. 116 (2012) 15231-15240.

[2] N. Ohba, et.al., Phys. Rev. B. 74 (2006) 075110.

## Disorder-Suppressed Vibrational Relaxation in Vapor-Deposited High-Density Amorphous Ice

Andrey Shalit<sup>1</sup>, Fivos Perakis<sup>1</sup>, Peter Hamm<sup>1</sup> \*

<sup>1</sup>University of Zurich

We apply two-dimensional infrared spectroscopy to differentiate between the two polyamorphous forms of glassy water – low-density (LDA) and high-density (HDA) amorphous ices, that were obtained by slow vapor deposition at 80 and 11 K respectively. High structural disorder and complete lack of spectral diffusion, intrinsic for the amorphous samples [1], allow one to observe variation in spectral properties of the uncoupled hydroxyl stretch vibration with hydrogen bond (HB) strength of surrounding water molecules. The vibrational lifetime ( $T_1$ ) of the isolated OD stretch (10% HDO in H<sub>2</sub>O) exhibits characteristic differences when comparing hexagonal ( $T_1=0.5$ ps), LDA ( $T_1=0.6$ ps) and HDA ( $T_1=1.6$ ps) ices under similar HB environment (i.e. same excitation frequency [2]), revealing reduced relaxation rate (by more than factor of 2) for the HDA. In addition the width of the 1-2 transition in HDA shows a reduced dependence on the excitation frequency when compared to LDA. We attribute these variations in the spectroscopic properties to the different local structures – in particular the presence of interstitial waters in HDA ice [3] – that cause different delocalization lengths of intermolecular phonon degrees of freedom. Temperature dependent measurements show that the vibrational lifetime of HDA ice decreases from 1.6 to 0.8 ps between 20 K and 40 K in a step-like manner, closely following its structural transformation to LDA ice around the same temperature [4].

[1] A. Shalit, F. Perakis and P. Hamm, *J. Phys. Chem. B.* **117** 15512 (2013)

[2] R. Rey, K. Møller, and J. T. Hynes, *J. Phys. Chem. A* **106**, 11993 (2002).

[3] J. L. Finney, A. Hallbrucker, I. Kohl, A. K. Soper, and D. T. Bowron, *Phys. Rev. Lett.* **88**, 225503 (2002).

[4] P. Jenniskens and D. Blake, *Science* **265**, 753 (1994)

**Reversible Isotope Exchange Reactions in Ca(BH<sub>4</sub>)<sub>2</sub>**

Manish Sharma<sup>1</sup>, Daniel Sethio<sup>1</sup>, Pascal Schouwink<sup>1</sup>, Radovan Černý<sup>1</sup>, Hans Hagemann<sup>1</sup> \*

<sup>1</sup>University of Geneva

Borohydrides are actively considered as potential hydrogen storage materials. In this context, the fundamental understanding of the mechanism of breaking and forming the boron-hydrogen bond is very important. Isotope exchange reactions allow in principle to isolate some parts of this reaction without having to consider the chemical and structural changes associated with thermal decomposition reactions. We have studied in the past [1] the reaction between Mg(BH<sub>4</sub>)<sub>2</sub> and D<sub>2</sub>(gas) at 40 bar and found an activation energy of 50 kJ/mol.

New experiments were performed on Ca(BH<sub>4</sub>)<sub>2</sub> and Ca(BD<sub>4</sub>)<sub>2</sub> as a function of temperature and pressure. The temperature ranged from 140 °C to 200 °C, and the D<sub>2</sub> (H<sub>2</sub>) pressure from 1 to 35 bar.

The experiments show that it is possible to entirely convert Ca(BH<sub>4</sub>)<sub>2</sub> to Ca(BD<sub>4</sub>)<sub>2</sub> and also that this reaction is reversible.

The activation energy estimated from first order kinetics of the forward reaction (Ca(BH<sub>4</sub>)<sub>2</sub> → Ca(BD<sub>4</sub>)<sub>2</sub>) was found to be 82.1 ± 2.7 kJ/mol (P = 35 bar), and the one for the backward reaction (Ca(BD<sub>4</sub>)<sub>2</sub> → Ca(BH<sub>4</sub>)<sub>2</sub>) was found to be 98.5 ± 8.3 kJ/mol (P = 35 bar).

Pressure dependent studies show that the reaction rate increases with increasing pressure up to 35 bars. This behavior is consistent with a first adsorption step prior to diffusion into the solid and isotope exchange according to the scheme:



Further, the reaction of BH<sub>4</sub><sup>-</sup> with deuterium radicals was studied theoretically using DFT calculations, yielding activation energy about 97 kJ/mol. This value is comparable to the experimental values and suggests that deuterium (hydrogen) radicals may indeed be involved in the isotope exchange reaction.

This work is supported by the Swiss National Science Foundation.

[1] Hans Hagemann, Vincenza D'Anna, J.P. Rapin, K. Yvon, *Journal of Physical Chemistry C*, **2010**, 114, 10045-10047.

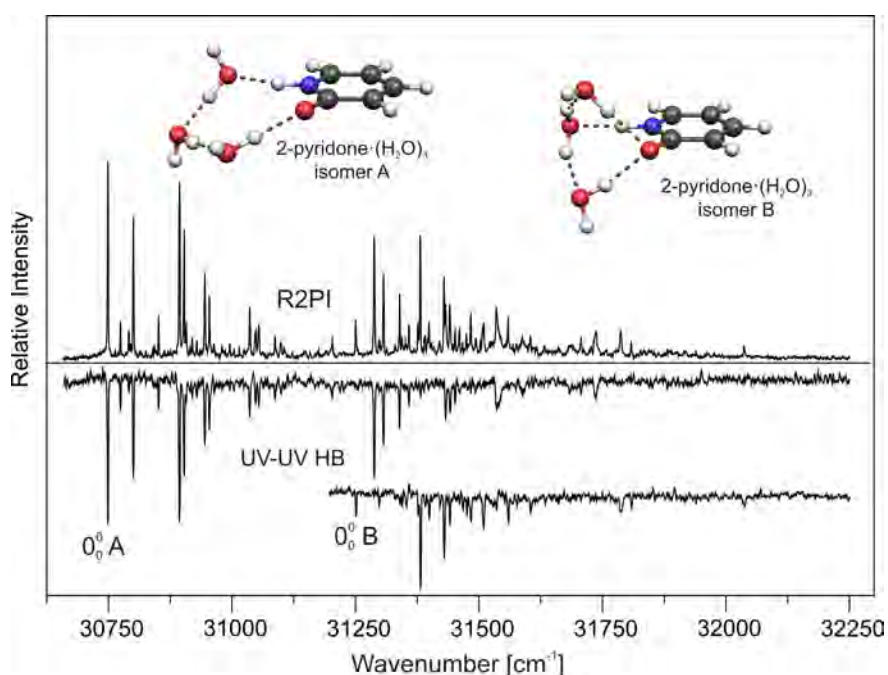
## Nanohydration of a Cis-Amide: Water Wires and Bridges

Luca Siffert<sup>1</sup>, Philipp Ottiger<sup>1</sup>, Susan Blaser<sup>1</sup>, Samuel Leutwyler<sup>1</sup> \*

<sup>1</sup>University of Berne

The mass-selective two-color resonant two-photon ionization (2C-R2PI) and infrared-depletion (IR) spectra of supersonic jet-cooled 2-pyridone-(H<sub>2</sub>O)<sub>n</sub> clusters with n = 1 - 4 have been measured to investigate the hydration pattern of a cis-amide UV chromophore. Additionally, UV-UV hole burning spectra of the n = 3 cluster have been recorded to identify two isomers A and B.

It is known that for n = 1 - 2, the clusters form a H-bonded single bridge structure.[1] Upon electronic excitation, the pyridone moiety remains planar due to the large contribution of quasi-ionic structures in contrast to the 2PY monomer.[2]



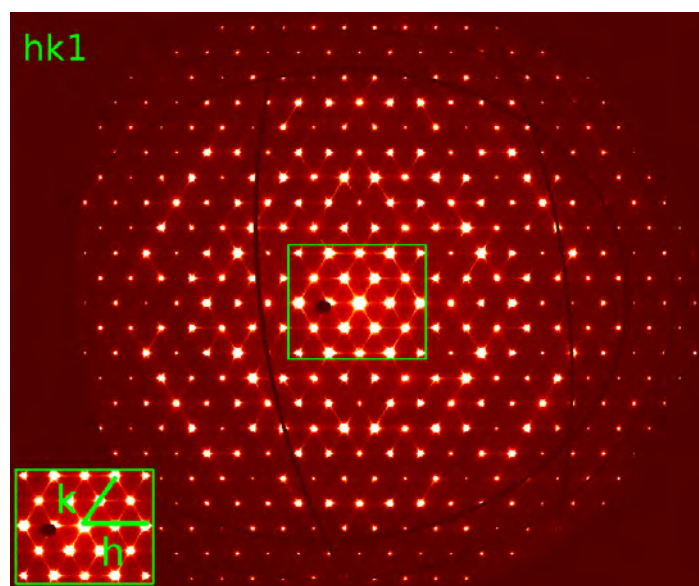
Our results revealed a second, bifurcated double bridged structure type for the n = 3 cluster with the same structural changes upon electronic excitation. For n = 4, only this isomer type has been detected. Corresponding SCS-RICC2 calculations show a correlation of the UV spectral shift of the origin band and the number of H-bonds to the keto group, which is in good agreement with experimental findings.

[1] G. Florio, C. Gruenloh, R. Quimpo, T. Zwier, *J. Chem. Phys.*, **2000**, 113, 24, 11143-11153

[2] R. Brause, M. Schmitt, K. Kleinermanns, *J. Phys. Chem. A*, **2007**, 111, 3287-3293

**Modelling diffuse scattering of the disordered crystal structure of Na<sub>2</sub>SiF<sub>6</sub>**Erik Stronks<sup>1</sup>, Hans-Beat Bürgi<sup>2</sup>, Anthony Linden<sup>1</sup>, Loes Kroon-Batenburg<sup>3</sup><sup>1</sup>University of Zurich, <sup>2</sup>University of Berne, University of Zurich, <sup>3</sup>Utrecht University

Many crystalline materials are not perfectly ordered, but are disordered to a smaller or larger extent. The properties of such materials are often related to the nature of the disorder. In diffraction experiments, disorder is observable as diffuse scattering. In routine X-ray structure determinations, only Bragg reflections are considered, leading to average crystal structure models. Methods to derive the average structure from the Bragg reflections are very well established, whereas diffuse scattering is rarely accounted for and mostly ignored. Our attempts at modelling the disordered structure of crystalline sodium fluorosilicate will be presented. Although the average crystal structure is known [1], there is some uncertainty about the true space group [2]. Na<sub>2</sub>SiF<sub>6</sub> assumes a crystalline morphology that resembles that of ice and is therefore known as an ice-analog material [3]. In the average crystal structure (in space group *P321*), the asymmetric unit contains two ordered sodium cations (both sitting on a two-fold axis) and two disordered SiF<sub>6</sub><sup>2-</sup> anions (one sitting on a 3-fold axis and the other on a 32 site). Each anion can occupy two alternative sites in the unit cell, related by a non-crystallographic mirror plane at  $z = \frac{1}{4}$ . The occupation is mutually exclusive for both anions. Diffuse scattering can be observed as planes perpendicular to  $l$  in the  $hnl$  and  $nk l$  precession images where these diffuse planes can be found at integer  $l$ . For  $l$  odd, the diffuse scattering is more intense. Also there are diffuse clouds of intensity around certain Bragg peaks. In the  $hkn$  planes, diffuse streaks are visible parallel to  $\mathbf{a}^*$ ,  $\mathbf{b}^*$ , and  $\mathbf{a}^* - \mathbf{b}^*$ , while some Bragg peaks have diffuse clouds of intensity around them. The pattern of streaks and clouds evolves when going to higher order planes. In the figure below, the  $hk1$  precession image is illustrated. The observed diffuse scattering features will be interpreted in terms of structural models obtained by Monte Carlo simulations.



[1] A. Zalkin, J. D. Forrester, D. H. Templeton, *Acta Cryst.*, 1964, 17, 1408.

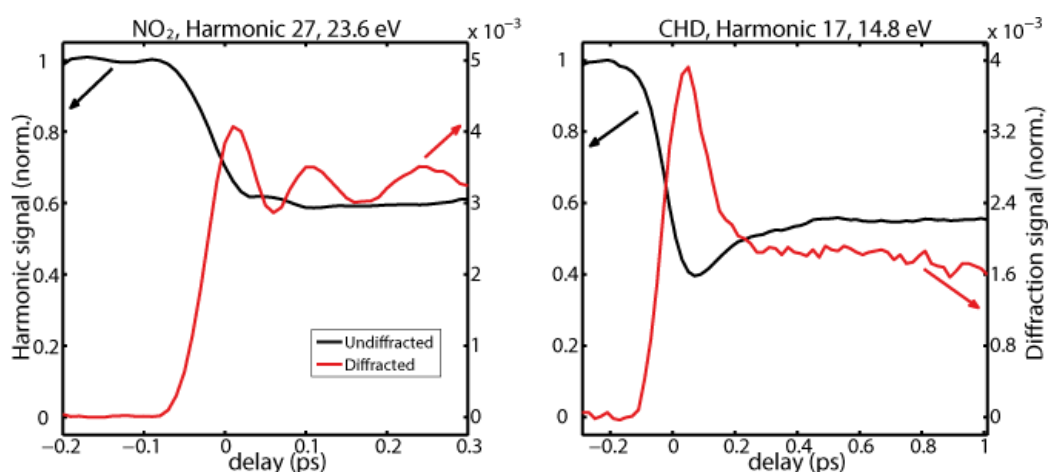
[2] G. F. Schäfer, *Zeitschrift für Kristallography*, 1986, 175, 269-276

[3] H. Jeong, Y. Huh, *Cryst. Materials Letters*, 2010, 64, 1816-1818

**Time-Resolved High-Harmonic Spectroscopy of conical intersection dynamics**Andres Tehlar<sup>1</sup>, Hans Jakob Wörner<sup>1</sup> \*<sup>1</sup>ETH Zurich

Conical intersections play an important role during chemical reaction dynamics. The ultrafast nature and complexity of the associated processes make their real-time observation very challenging. We present the results of two case studies of photoreactions involving conical intersections: The photodissociation of NO<sub>2</sub> after excitation at 397 nm and the ring-opening of 1,3-cyclohexadiene (CHD) at 267 nm. High-harmonic emission is known to be very sensitive to the electronic structure, which makes it a prime candidate to observe the temporal variation of the electronic character. We excited the molecules in a transient grating setup, crossing two pump beams under a small angle in the focus. The temporal variation of the high-harmonic emission from the photoexcited molecules is detected with high sensitivity through diffraction in the far field. In NO<sub>2</sub>, we observe a damped oscillation, characterizing the oscillations of the electronic molecular character between <sup>2</sup>B<sub>2</sub> and <sup>2</sup>A<sub>1</sub> during the first 200 fs of the dissociation (see figure below, left panel). The undiffracted signal (black, left scale) drops after delay zero between the pump and the high-harmonic generating probe (1420 nm), and shows weak modulations afterwards. The diffracted signal (red, right scale) increases after time zero and shows a strong oscillation, which is out of phase with the undiffracted one. In CHD, we find a fast variation of the emitted intensity over the first 200 fs, which can be attributed to the wave-packet motion from the 1B over the 2A to the 1A surface of the 1,3,5-hexatriene product (see figure, right panel). The undiffracted signal shows a sharp drop after delay zero between pump (266 nm) and the high-harmonic generating probe, recovering partially within 600 fs. The diffracted signal shows a similar, but opposite moving behavior.

Further, we present first results on the impulsive alignment of CHD in order to follow the reaction in the molecular frame. We compare the full rotational revivals of CHD to benzene. We find striking differences between the two molecules that we rationalize in terms of the photorecombination matrix elements of the inner and outer valence orbitals of CHD.

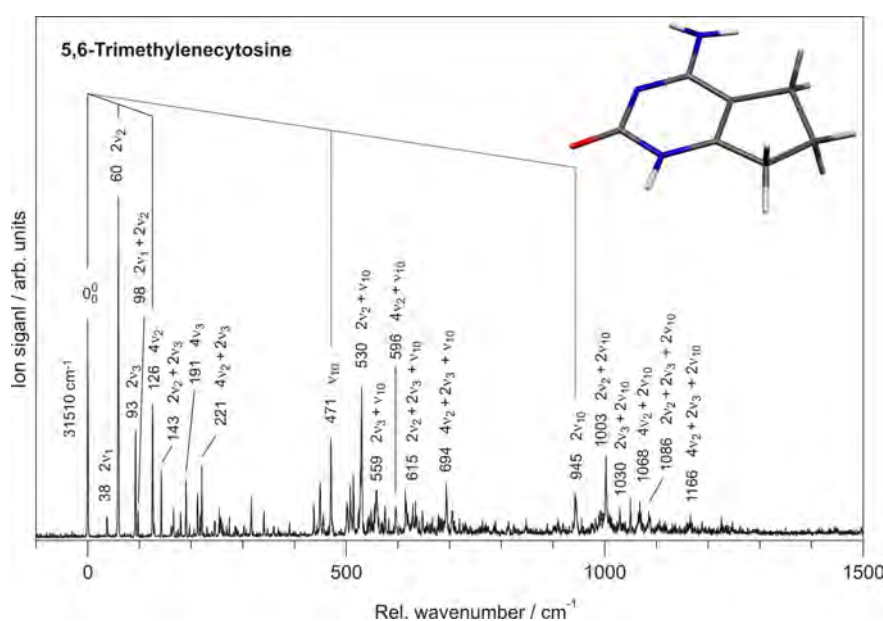


## Supersonic Jet UV Spectra and Nonradiative Relaxation of Methylated Cytosines

Maria Trachsel<sup>1</sup>, Simon Lobsiger<sup>1</sup>, Samuel Leutwyler<sup>1</sup> \*

<sup>1</sup>University of Berne

We have measured the vibronically resolved two-color resonant two-photon ionization spectra of jet cooled 5-methylcytosine (5MCyt) [1], 6-methylcytosine (6MCyt) and 5,6-trimethylenecytosine. The threshold for internal conversion (IC) from the  $S_1$  state to the ground state can be closely estimated from the breakoff of the vibronic spectrum as  $500\text{ cm}^{-1}$  for cytosine (Cyt) [2],  $\sim 200\text{ cm}^{-1}$  for 6MCyt and  $\sim 600\text{ cm}^{-1}$  for 5MCyt. [1] Obviously, methylation at the  $C^5=C^6$  double bond does not significantly influence the  $S_1 \rightarrow S_0$  IC threshold. In contrast, 5,6-trimethylenecytosine has a much higher IC threshold of  $\sim 1250\text{ cm}^{-1}$ . Bridging the 5- and 6-positions with an aliphatic ring strongly hinders the access to the low-energy  $C^6$ -twist conical intersection in the  $S_1 \pi\pi^*$  state.



[1] M. A. Trachsel, S. Lobsiger and S. Leutwyler, *J. Phys. Chem. B*, **2012**, 116, 11081.

[2] S. Lobsiger, M. A. Trachsel, H.-M. Frey and S. Leutwyler, *J. Phys. Chem. B*, **2013**, 117, 6106.

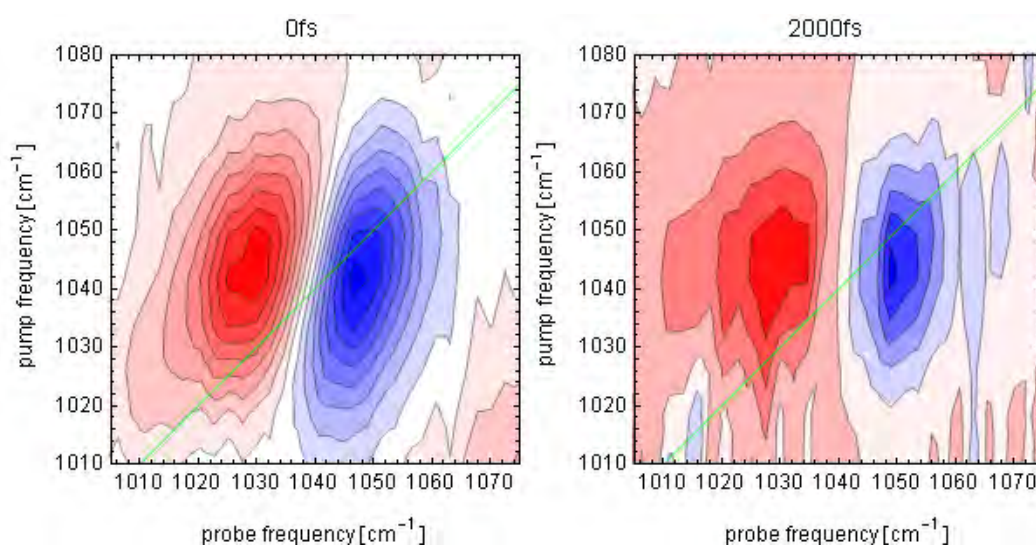
## The Solvated Carbon-Fluorine Bond in Water Investigated by 2D IR spectroscopy

Halina Tran<sup>1</sup>, Peter Hamm<sup>1</sup> \*

<sup>1</sup>University of Zurich

Organic fluorinated molecules are very rare in nature, however 20-25% of current drugs contain at least one fluorine atom [1]. The interactions of the C-F bond with surrounding water molecules play an important role in the functionality of fluorinated drugs.

We investigate this intermolecular coupling utilizing two-dimensional infrared spectroscopy on the femtosecond time scale. The two-dimensional line shape of the C-F band gives information about the dynamics of the surrounding, especially through the decay of the nodal line slope that is caused by spectral diffusion of its inhomogeneous frequency distribution [Fig].



Fluoroacetonitrile (F-ACN) was chosen as a model system, because it has a simple infrared absorption spectrum and exists as a single conformer - however it is a relatively weak absorber ( $\epsilon \sim 50 \text{ M}^{-1} \text{ cm}^{-1}$ ). We used NMR studies to determine the maximum sample concentration at which the system can still be considered to be dilute (200 mM F-ACN in D<sub>2</sub>O). We observe that the tilt of the 2D-IR line-shape as a function of population time decays with a lifetime of  $\tau = 0.6$  ps. In analogy to a recent study [2,3] our results can be used to further test and develop molecular dynamics force fields to better describe the solvation properties of fluorinated molecules.

[1] S. Purser, P. R. Moore, S. Swallow, V. Gouverneur, *Chemical Society Reviews*, **2008**, 37, 320-330.

[2] M. Koziński, S. Garrett-Roe, P. Hamm, *Chemical Physics*, **2007**, 34, 5-10.

[3] M. W. Lee, J. K. Carr, M. Göllner, P. Hamm, M. Meuwly, *The Journal of Chemical Physics*, **2013**, 139, 054506.

## Alignment effects in the dissociative chemisorption of methane: the role of vibrational symmetry

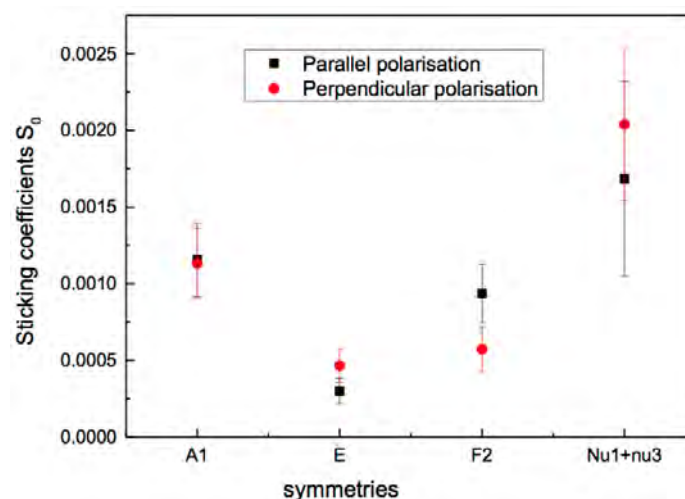
Maarten van Reijzen<sup>1</sup>, Phil Morten Hundt<sup>1</sup>, Helen Chadwick<sup>1</sup>, Rainer Beck<sup>1</sup> \*

<sup>1</sup>EPFL Lausanne

Steric effects for bimolecular reactions in the gas phase have been studied in great detail by crossed molecular beam experiments for several decades. The latest experiments[1] show distinctly different reaction pathways for differently aligned collision geometries. For gas-surface reactions, an alignment dependence of the reactivity of the incident reactants on the solid surface has only recently been uncovered. For the dissociative chemisorption of methane on a nickel surface, our group has previously discovered an alignment effect where the reactivity is highest when the vibrational transition dipole moment is aligned parallel to the plane of the surface both for  $\text{CH}_4(\nu_3)$  and  $\text{CHD}_3(\nu_1)$ [2].

In this work, we continue our investigation of alignment effects for methane dissociation on Ni(111) for the  $2\nu_3$  overtone vibrations, which are split into three nearly iso-energetic symmetry components  $A_1$ , E and  $F_2$ , as well as for the  $\nu_1+\nu_3$  combination vibration. Using linearly polarized light from two continuous wave optical parametric oscillators (CW-OPO), we align the molecules in the laboratory frame just before collision with a Ni(111) single crystal. By rotating the electric vector of the linearly polarized light  $90^\circ$ , we prepare alignment configurations of the C-H stretch amplitude, both parallel and perpendicular with respect to the plane of the surface. Dissociation products are detected and quantified using Auger electron spectroscopy. Incident reactant flux is measured using a calibrated quadrupole mass spectrometer. We analyze these two measured quantities to yield the quantum state resolved sticking coefficient  $S_0$  as a function of the laser polarization direction.

Our results show a significant alignment effect for both the excited E and  $F_2$  vibrational symmetry components of  $2\nu_3$ , whereas the totally symmetric  $A_1$  and the  $\nu_1+\nu_3$  combination do not show any alignment dependence in the dissociation probabilities. Interestingly, the E and  $F_2$  symmetry show opposite alignment effects for the two applied alignments, as can be seen in the figure below. Where the  $F_2$  symmetry has a higher sticking coefficient for the laser polarization aligned parallel to the surface, the E symmetry has a higher sticking coefficient for perpendicular alignment. In our contribution, I will present a detailed analysis of the alignment effects for the different  $2\nu_3$  vibrational states of  $\text{CH}_4$ .



[1] Wang F., K. Liu, T.P. Rakitzis, Nature Chemistry (2012), 4, 636

[2] Yoder B.L., R.Bisson, R.D. Beck, Science, (2010) 329, 553

## A high-flux femtosecond XUV beamline for time-resolved photoelectron spectroscopy.

Aaron von Conta<sup>1</sup>, Hans Jakob Wörner<sup>1</sup> \*

<sup>1</sup>ETH Zurich

We will describe the design and operation of a high-flux femtosecond XUV beamline for time-resolved photoelectron spectroscopy. A time-preserving XUV/VUV monochromator for HHG radiation [1] based on the principle of conical diffraction [2] is combined with a semi-infinite gas cell [3]. This device delivers the radiation corresponding to a single harmonic order with a moderate temporal broadening ( $\leq 15$  fs) compared to the pulse duration of the laser pulse driving the XUV generation process. The obtainable photon energies lie in the range between 10 eV and 100 eV, where the upper limit is defined by the laser driving the XUV source. We are presenting a first cross-correlation of the XUV radiation obtained in a magnetic-bottle spectrometer. Evidence for a very high photon flux of the order of  $10^{12}$  photons per second at 30 eV will be presented. This number is by a factor of 100 larger than values reported from other existing high harmonic generation based monochromator beamlines. The measured flux is consistent with previous data published for semi-infinite gas cell driven XUV sources [3] and for the comparably high transmission ( $\approx 40\%$ ) reported for this type of monochromator [1].

The monochromator will ultimately be used in combination with a velocity-map-imaging (VMI) spectrometer, to study the femtosecond dynamics of a small polyatomic molecules. We expect that XUV time-resolved photoelectron spectroscopy will provide considerable new insight into the rich photochemical processes occurring in these species. It will also provide reference measurements for time resolved high-harmonic spectroscopy [4] by making angular resolved one-photon ionization cross sections experimentally available. In the future, we will use the monochromator as light source for liquid-jet photoelectron spectroscopy, which will allow us to systematically vary the probe depth at liquid-solid interfaces.

[1] F. Frassetto et al., Opt. Exp., **2011**, 19.20, 19169.

[2] W. Cash, Appl. Opt., **1982**, 21, 710.

[3] J. Sutherland et al., Opt. Exp., **2004**, 12, 4430.

[4] H. J. Wörner et al., Science, **2011**, 334, 208.

**Imaging Electronic Wave Packets Through Electron Rescattering and Holography**

Samuel Walt<sup>1</sup>, N. Bhargava Ram<sup>1</sup>, Hans Jakob Wörner<sup>1</sup> \*

<sup>1</sup>ETH Zurich

We demonstrate a new experimental method to observing electronic wave-packet motion. Impulsive stimulated Raman excitation has been used to prepare a coherent superposition of the  $^2\Pi_{1/2}$  and  $^2\Pi_{3/2}$  states of nitric oxide. The resulting electronic wave packet corresponds to an electron density rotating around the molecular axis with a period of 278 femtoseconds. A time-delayed intense laser pulse was used to transfer the excited electron into the continuum where its motion is dominated by the oscillating electromagnetic field of the laser pulse. The trajectories of this motion can include an elastic scattering process with the parent ion. The interference between electrons reaching the detector directly and those rescattering once give rise to “holographic” structures in the final momentum distribution of the photo electrons. The momentum distribution of photoelectrons was measured with a velocity map imaging spectrometer. We observe a modulation of the holographic structure as a function of the pump-probe delay as a consequence of the electronic wave packet motion. This modulation is absent in the rescattered electrons themselves, which however reveal the rotational wave-packet dynamics of the molecule. This allowed us to observe the two simultaneously occurring wave-packet motions in complementary observables.

**The  $\beta$ -phase of Pigment Red 170: Faulted stacking of 2D periodic molecular layers.**

Rangana Warshamanage<sup>1</sup>, Anthony Linden<sup>2</sup>, Hans-Beat Bürgi<sup>3</sup>

<sup>1</sup>University of Zurich, <sup>2</sup>University of Zurich, <sup>3</sup>University of Berne, University of Zurich

The single-crystal X-ray diffraction pattern from the  $\beta$ -phase of the industrially important Pigment Red 170 ( $\beta$ -P.R.170) is extremely complicated thus illustrating the complexity of real life crystals which are a far cry from the regular arrangement of unit cells given in text books and present a big challenge to X-ray crystallography. The diffraction pattern consists of a difficult-to-disentangle mixture of Bragg diffraction superimposed by rods of diffuse scattering and satellite peaks. The analysis of only Bragg scattering has shown that this compound does not have one, but two plausible average structures [1]. The analysis of diffuse scattering, which is a signature of the interactions between neighboring layers of this material, is carried out with the help of extensive Monte Carlo simulations combined with evolutionary algorithms [2]. The analysis so far has shown that the nearest-neighbor interactions between layers can reproduce the diffraction pattern only qualitatively. Furthermore, carefully processed experimental profiles show a fine structure of additional peaks (satellites) positioned around the Bragg peaks implying that there may also be a modulation in the structure. The magnitude of these signals is approximately of the same order of magnitude as that of the Bragg signals implying that  $\beta$ -P.R.170 is an extreme example of stacking faults. Our current focus is on analyzing the position and intensity of the satellite peaks in the diffraction data and obtaining an optimal set of interaction parameters that describe the most favorable interactions between layers.

- [1]. R. Warshamanage, A. Linden, M.U. Schmidt, H.-B. Bürgi, *Acta Cryst. B*, **2014**, 70, 283-295.  
[2]. T. Weber, H.-B. Bürgi, *Acta Cryst. A*, **2002**, 58, 526-540.

**Studying structure disorder in DL-Norvaline by single crystal diffuse scattering**Jun Xu<sup>1</sup>, Anthony Linden<sup>1</sup>, Hans-Beat Bürgi<sup>2</sup><sup>1</sup>University of Zurich, <sup>2</sup>University of Berne, University of Zurich

Real materials are often not perfectly ordered. The diffraction pattern always contains sharp Bragg peaks and a weak continuous or structured background known as diffuse scattering. Our motivation is to learn about the Short Range Order (SRO) of disordered crystals and improve the tools to model disorder phenomena. We are now investigating the SRO in DL-Norvaline which crystallizes in three known temperature-dependent phases. At least two of them ( $\beta$ -phase space group  $C2/c$  above  $-70^\circ\text{C}$ ,  $\alpha$ -phase  $P2_1/c$  around  $-90^\circ\text{C}$ ) show disordered average structures [1]. Due to the weakness of the diffuse scattering signal, the scattering data were collected using synchrotron radiation and a noise-free Pilatus pixel detector at the ESRF BM01A station. The diffraction pattern of the  $\beta$ -phase shows diffuse streaks parallel to a reciprocal lattice axis and diffuse clouds around low angle reflections[2] (Fig. 1). The diffuse streaks indicate disorder amongst stacks of layers of molecules, while the diffuse clouds arise from thermal motion. The current study shows that randomly distributed disordered layer arrangements arise because the disordered alkyl side chain rearranges entirely during martensitic transformations. The quantitative analysis of the structure disorder and diffuse scattering is currently underway and involves the use of the Monte Carlo and differential evolution algorithms embedded in ZODS [3].

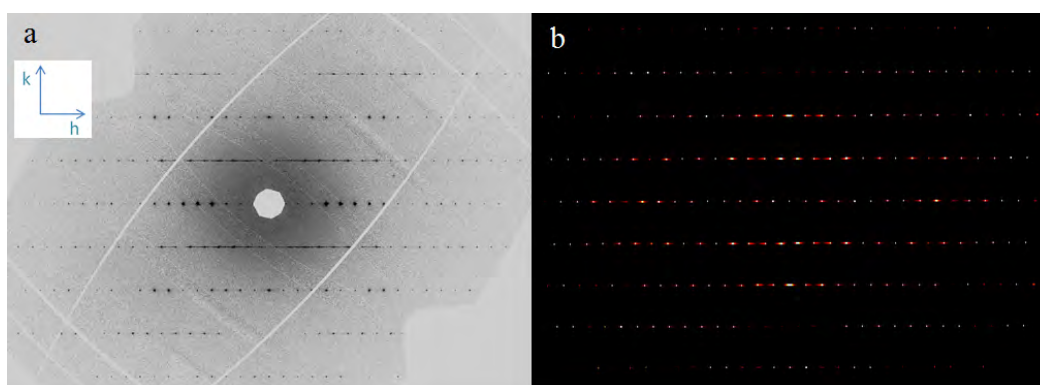


**Figure 1.** Diffuse scattering in the  $hk0$  layer. (a) Experimental pattern (b) Simulated pattern

[1] C.H. Görbitz, *J. Phys. Chem. B* **2011**, 115, 2447.

[2] Agilent Technologies (**2012**). CrysAlisPro, Agilent Technologies, Yarnton, Oxfordshire, England.

[3] ZODS: Zurich-Oak Ridge Disorder Simulation software, ETH/UZH, under development.



## Continuous trap loading of Rydberg atoms and molecules using overlaid electric and magnetic traps

Matija Zesko<sup>1</sup>, Christian Seiler<sup>1</sup>, Frédéric Merkt<sup>1</sup> \*

<sup>1</sup>Laboratory of Physical Chemistry, ETH Zurich, 8093 Zurich, Switzerland

The technique of Rydberg-Stark deceleration has provided a means to decelerate and trap Rydberg atoms and molecules at a temperature of around 100 mK. This technique relies on the very large electric dipole moments of Rydberg-Stark states (up to 3000 D at  $n=30$ ) which enable one to exert large deceleration forces on atomic and molecular beams using inhomogeneous electric fields.

In the case of atomic hydrogen and helium at  $n=30$ , the trapped Rydberg atoms decay by fluorescence on a time scale of around 100  $\mu\text{s}$  [1, 2]. This decay opens up the possibility to trap paramagnetic atoms in their ground state or a metastable state using an overlaid electric and magnetic trap. Such a trap would offer the advantage of increasing the phase-space density of the trapped atoms by accumulating population in the ground state in successive experimental cycles. To achieve this goal, a new experimental setup has been designed and constructed with which metastable He ( $1s)(2s) \ ^3S_1$ ) can be trapped magnetically following Rydberg-Stark deceleration.

The He Rydberg atoms are prepared in a selected Rydberg-Stark state using a home-built narrow-bandwidth (160 MHz) pulsed tunable laser. The Rydberg atoms are then decelerated and deflected from the atomic beam axis and trapped electrostatically as described in [3]. Currently, we are testing how magnetic fields such as those that will be required to trap the atoms magnetically influence the Rydberg-Stark states and the deceleration process.

[1] S. D. Hogan, and F. Merkt, *Phys. Rev. Lett.*, **100**(4), 043001, (2008.)

[2] P. Allmendinger, J. A. Agner, H. Schmutz, and F. Merkt, *Phys. Rev. A*, **88**(4), 043433, (2013.)

[3] Ch. Seiler, S. D. Hogan, H. Schmutz, J. A. Agner and F. Merkt, *Phys. Rev. Lett.*, **106**(7), 073003, (2011.)

## Placing Nanosheets on Graphene

Zhikun Zheng<sup>1</sup>, Lothar Opilik<sup>1</sup>, Wyss Roman<sup>1</sup>, Hyung Gyu Park<sup>1</sup>, Renato Zenobi<sup>1</sup>, A. Dieter Schlüter<sup>1</sup> \*

<sup>1</sup>ETH Zurich

Graphene, an atomic layer of graphite, has gained a deep scientific and even social interest due to its unique physical and chemical properties, which derive from its  $\pi$ -conjugated system of  $sp^2$ -bonded carbons. However, the conjugation makes graphene surface chemically inert, which poses great challenges for its integration in devices. Covalent functionalization of graphene provides a way to meet the challenge, however it converts  $sp^2$ -bonded carbons to  $sp^3$ -bonded ones, which disrupts the intrinsic structure of graphene, from which most of the desirable properties of graphene arise. Non-covalent adsorption of active materials onto graphene surface provides another way to meet the challenge, however non-covalently adsorbed materials are easily desorbed from graphene surface by organic solvent rinsing, thermal annealing or with time. We present here the challenge can be well addressed by placing nanosheets that are capable to bond with graphene with multivalent non-covalent interactions.<sup>1-4</sup> The nanosheets can be either used to turn the band gap of graphene or as adhesive layers for its integration in devices, such as in capacitors. The placing of nanosheets on graphene opens the door for its integration in electronic, photovoltaic, and sensing devices without disrupting its intrinsic structure and thus the properties.

(1) Bauer, T.; Zheng, Z.; Renn, A.; Enning, R.; Stemmer, A.; Sakamoto, J.; Schlüter, A. D. *Angew. Chem., Int. Ed.* **2011**, *50*, 7879-7884. (2) Zheng, Z.; Ruiz-Vargas, C. S.; Bauer, T.; Rossi, A.; Payamyar, P.; Schütz, A.; Stemmer, A.; Sakamoto, J.; Schlüter, A. D. *Macromol. Rapid Commun.* **2013**, *34*, 1670-1680. (3) Zheng, Z.; Opilik, L.; Schiffmann, F.; Liu, W.; Bergamini, G.; Ceroni, P.; Lee, L.; Schütz, A.; Sakamoto, J.; Zenobi, R.; VandeVondele, J.; Schlüter, A. D. *J. Am. Chem. Soc.* **2014**, *136*, 6103-6110. (4) Chen, Y.; Li, M.; Payamyar, P.; Zheng, Z.; Sakamoto, J.; Schlüter, A. D. *ACS Macro Lett.* **2014**, *3*, 153- 158.

**Molecular dynamics simulations of ion pairing in water**

Ganna Berezovska<sup>1</sup>, Myung Won Lee<sup>2</sup>, Markus Meuwly<sup>2</sup> \*

<sup>1</sup>Albert-Ludwigs University of Freiburg, <sup>2</sup>University of Basel

The reorientation dynamics of water molecules around ions take place on a *ps* time scale and is important in many chemical and biological applications such as ion transport through membrane or solubility of other molecules in solution. However, understanding of hydration shell dynamics on a microscopic level is not complete suggesting two competitive scenarios: Prevailing role of disruption of a hydrogen-bond network around ions or dominating of ion-water interactions. Experimental studies of different electrolyte solutions show that this results in either increasing or decreasing of the water self-diffusion coefficient with concentration, the trend which have not been captured so far by MD simulations with any force field<sup>[1]</sup>. Here we would like to revisit the problem exploring a performance of the CHARMM force field with multipolar approach for electrostatic interactions<sup>[2]</sup>, that have not been done before. We test the simulation approach on a number of systems such as solvated cyanide<sup>[3]</sup>, KBr and NaBr in water.

[1] Jun Soo Kim, Zhe Wu, Andrew R. Morrow, Anand Yethiraj, Arun Yethiraj, *J. Phys. Chem. B* **116**, 12007 (2012)

[2] N. Plattner, M. Meuwly, *Biophys. J.* **94**, 2505 (2008)

[3] Myung Won Lee, Joshua K. Carr, Michael Göllner, Peter Hamm, Markus Meuwly, *J. Chem. Phys.* **139**, 054506 (2013)